VOL. XXI

REVIEW OF THE AIR FORCE ACADEMY

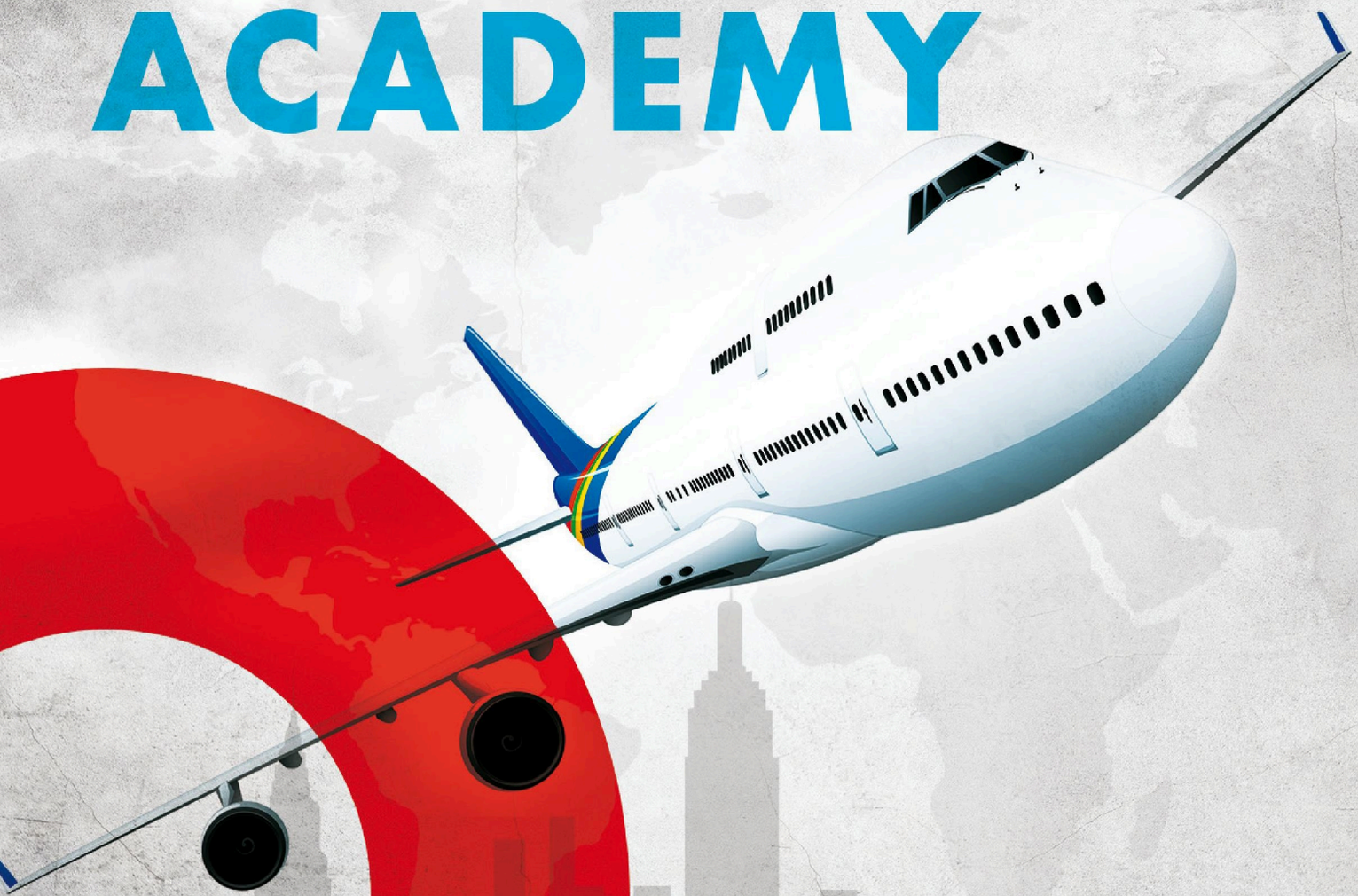

No. 1 (47)/2023

Review
of the Air Force Academy

The Scientific Informative Review, Vol. XXI, No.1 (47)/2023
DOI: 10.19062/1842-9238.2023.21.1

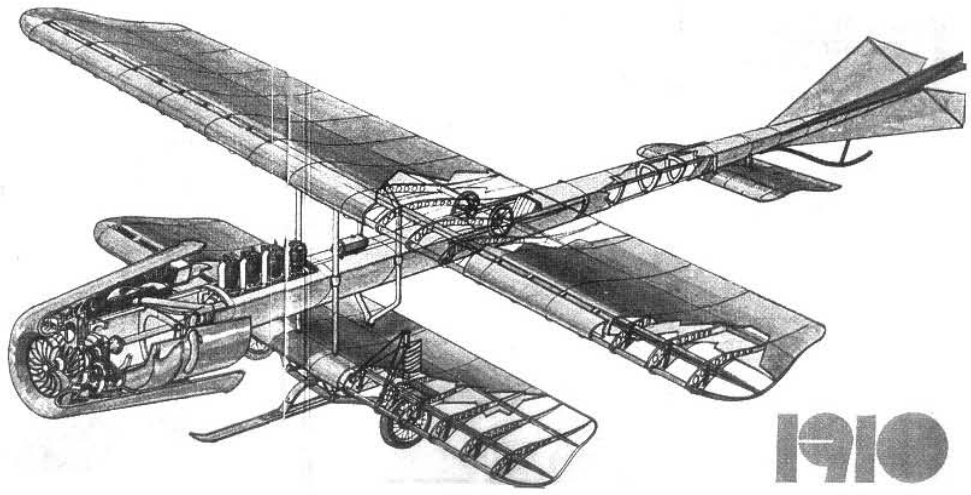

BRAŞOV - ROMANIA

© October, 2023
Visa 0574-10/2023
I.S.S.N. 1842-9238

"Henri Coandă" Air Force Academy Publishing House, 160, Mihai Viteazul St., Brașov, ROMÂNIA
Phone: +40 268 423421, e-mail: editura@afahc.ro

C O N T E N T S

DESIGN, ANALYSIS AND 3D PRINTING OF A MORPHING WING PROTOTYPE

Lucian-Nicolae BAJZAT
"Transilvania" University of Braşov, Romania (lucian-nicolae.bajzat@student.unitbv.ro)

Sebastian-Marian ZAHARIA
"Transilvania" University of Braşov, Romania (zaharia_sebastian@unitbv.ro)
ORCID: 0000-0002-8636-5558

DOI: 10.19062/1842-9238.2023.21.1.1

Abstract: *In this study, two different wing morphing models were chosen for design and testing. The selected models allow for significant considerations due to their airfoil geometry variation and wingspan variation. The purpose of choosing these prototypes was to highlight the benefits of the morphing wing concept as applied to aircraft, and further applied to UAVs, as well as to light and ultra-light aircraft. In order to confirm these advantages that support the reasons for applying the concept, both structural and aerodynamic analyses were carried out. Finally, the morphing wing model with chord extension was physically manufactured by means of a 3D printing process and tested to validate the proposed concept.*

Keywords: *wing morphing, CFD analysis, finite elements analysis, 3D printing*

1. INTRODUCTION

Morphing can be defined as the ability to transform or change the shape or nature of an aircraft structure. When applied to an aircraft, this concept refers to the ability to change the shape of the wing during flight while providing an important aerodynamic advantage [1].

This change in shape occurs according to the flight mission of the aircraft or according to its flight conditions. In this way the morphing wing is defined as a wing with the capability of continuous shape change in the longitudinal plane (along the spars) or in the transverse plane (along the chord), being able to achieve this shape change in a drastic manner [2,3].

While active morphing defines the change of flight configuration through the actions of the autopilot or ground station, passive morphing refers to cases where the aerodynamic configuration is modified without the action of the autopilot or other operator [4,5].

Nowadays, 3D printing equipment is increasingly used in many fields, including engineering. Given the market and industry need, the advantages that this manufacturing process offers (reduced manufacturing time, varied additive materials, cost reduction, design optimization by using various types of fill density configurations) are the best argument for using this technology in aviation [6,7].

As expected, this technology has also been used in the aerospace industry being typically used to manufacture prototypes for parts that do not have a crucial structural role or even for ground-operated aircraft such as drones [8] and unmanned aircraft [9].

Because of the advantages of this technology, 3D printing has also been used for morphing designs. Through 3D printing of the CAD model, both 2D morphing concepts with profile modification and, more specifically, 3D concepts can be created [10,11].

2. MORPHING WING DESIGN

In order to design a morphing wing, it is necessary to take into account and consider two very important aspects: shape modification characteristics - a morphing structure must allow a well-defined shape modification, in relation to the limits of the forces acting on the model in question; structural integrity - the structure of a morphing wing differs from a conventional wing precisely by its properties of elastic shape modification. However, the designer must ensure the integrity of the assembly because it must withstand the applied stresses without buckling, fatigue or flutter. Often these two requirements are in conflict and a compromise solution must be found [12].

In order to find and implement the best option, it has been concluded that the best materials to be used in the manufacture of morphing wings are composite materials [13,14]. Composite materials have very good properties in terms of fibre orientation variation, the stiffness distribution can be adapted to cope with bending stresses. Composite materials also meet the divergence requirements in both the wingspan and chord extension directions [13,14].

Considering these aspects, two different morphing models were chosen for analysis in this paper. The first model is based on the modification of the wing geometry in terms of the aerodynamic mean chord giving a higher airfoil efficiency (Fig. 1a), and the second model shows a longitudinal extension by increasing the wingspan (Fig. 1b).

These two models use a technology that helps to achieve extension through a mechanical and an electrical system. Furthermore, the materials used are also of prime importance, as they must develop excellent elastic, thermal, physical, and mechanical properties, as they play an essential role in the designed assembly.

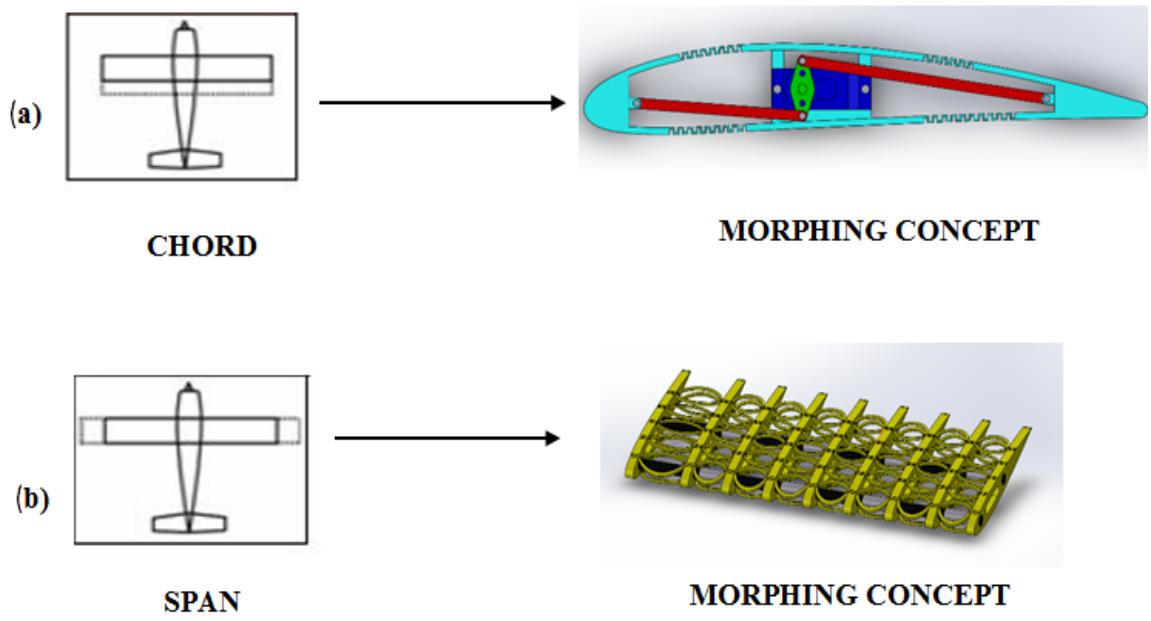

FIG. 1 Designed morphing wing models: (a) morphing model with chord extension, (b) morphing model with span extension

Morphing wing with variable (chord) profile (Fig. 2) - depending on the type and direction of deformation, this model falls into those whose aerodynamic mean chord is modified. The consequence of this modification is the increase or decrease of the aerodynamic mean chord of the model and at the same time the deformation of the airfoil from its initial position to one that gives the wing a concave or convex appearance.

In this way, by changing the airfoil shape, the wing can generate more lift when needed (usually in take-off and landing or at low speeds). For the design of this model, the NACA 4412 airfoil was initially chosen because of its good lift coefficient ratio.

The model has a length of 150 mm and a thickness of 2 mm, and the chord of this section measures 180 mm (Fig. 2a). These dimensions have been chosen in order to simplify the 3D printing procedure and at the same time to demonstrate the working principle and the benefits of the model in order to apply he prototype for a UAV.

The material chosen for this morphing wing prototype, of which the section was designed, is Nylon Alloy 910. It has excellent both physical and mechanical properties, providing extra safety to the structure. On the other hand, it also gives the elasticity needed to deform the model without suffering any defects because of this elastic deformation. To modify the shape of this prototype, a digital servo was used as the source of the mechanical system.

This digital servo is positioned on the specially designed support. The digital servo has 2 parts that have been designed: the body itself and the digital servo arm. The connections forming the chain drive from the digital servo to the designed model are represented by 2 arms. These are connected at one end by the last holes of the servo arm and at the other end by the model fasteners, thus forming the mechanical extension chain of the designed model (Fig. 2b).

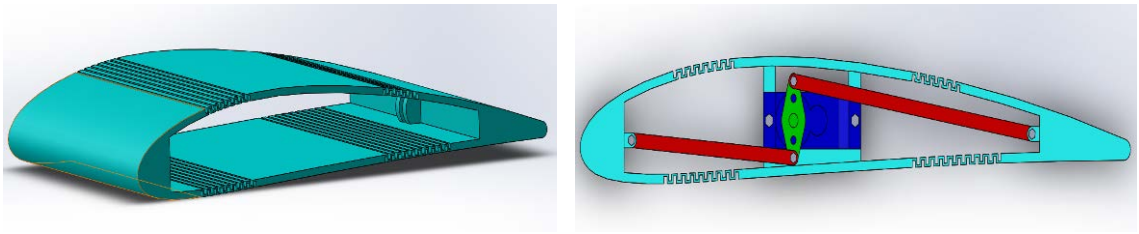

(a) (b)

FIG. 2 Variable chord morphing wing model: (a), intermediary model (b) final model

Variable span morphing wing - this model aims to lengthen the span by 12.3% from the current compressed state to the extended state (Fig. 3). Wingspan extension takes place in 4 gradual steps of equal elongation. This concept has been designed considering the stiffness of the assembly following this deformation and precisely because of this, the elongation percentage is not very high, keeping the structure rigid and safe.

The structure of this concept is made up of the following elements: 9 ribs, 4 groups of 2 ribs at symmetrical distances from each other and the ninth at a greater distance from the last group, at the tip of the wing; two cylindrical spars (main and secondary) which were also divided into 10 elements in order to place the linear actuators in those areas; the linear actuators are used to drive the longitudinal segments, making them slide and increasing the span.

There are 8 of them, positioned between the 4 pairs of ribs on both the main and secondary spars; the elastic bands maintain the shape of the ribs and stiffen the model, but also provide an additional elastic aid (20 corrugated honeycomb elastic bands); the shell is made of a thin latex film, which is a material with ideal elastic, mechanical and physical properties for this type of elastic deformation, with no risk of breakage in this case.

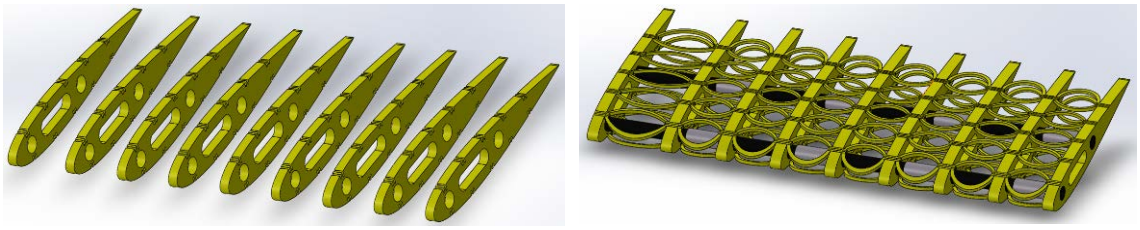

(a) (b)

FIG. 3 Variable span morphing wing model: (a) intermediary model (b) final model

In order to change the wing span, 8 piezoelectric linear actuators were used as motion sources and positioned in the area of the spar sections. The piezoelectric linear actuators are usually used in scientific and industrial applications, where high precision in motion control is required. These actuators are well known because they are often used in all modern high-tech fields including microscopy, bio-nanotechnology [15] and aerospace engineering [16,17].

3. FINITE ELEMENT ANALYSIS OF THE WING STRUCTURE

3.1 Finite element analysis of morphing wing with a variable profile

For this wing morphing concept, the finite element analysis was chosen to get results regarding the modification of the profile of the designed prototype from the initial state to the state of maximum deformation. The main goal of this morphing wing design is its future application to UAV-type aircraft or even to some ultra-light aircraft. In order to obtain relevant results in this direction, the designed prototype was scaled by a ratio of 1:6. This resulted in a wing segment with an aerodynamic profile whose chord measures 1080 mm and 900 mm in wingspan, a size close to those found on aircraft in the above-mentioned target classes. As a first step, Ansys 16.0 was chosen as the software system in which to perform these finite element analyses. The meshing of the model was carried out with an element size of 5 mm, totaling in the end 323322 elements joined by 600712 nodes. After the prototype was meshed, the fixing surfaces that will have non-deformable behavior at the analysis level and the surfaces on which the established forces are applied were determined. The fixing surface was chosen as the support of the digital servos acting on the whole wing profile modification system.

Regarding the materials used in these analyses, 3 different types of materials were selected with excellent properties in terms of flexibility and elasticity, which facilitate the deformation of the model much more easily. The materials chosen are Nylon Alloy 910, Flexifill 92A and Nylon CF 15. These materials have been added to the FEA software system by inserting some basic parameters to get the required characteristics. Since the motion generated by the digital servo gives both a concave (Fig. 4a) and a convex (Fig. 4b) deformation of the profile, both cases were analyzed.

As it can be seen, the central area is the stiffest because this is the fastened area where the digital servo is positioned. The total displacements obtained (Fig. 4c) expand in proportion to the distance from this fastening area, the maximum values being found at the model fasteners where the force is transmitted to the model. The total displacements obtained (Fig. 4d), for the convex case are about 50% smaller than in the first phase (concave case). This was predictable and natural considering that the aim of this displacement is to obtain, first of all, a part which will generate a lift force as high as possible in relation to the generated drag.

Regarding the equivalent stresses (Fig. 4e and Fig. 4f), the values are close, and for the two cases of analysis, the models withstand the applied stresses as they do not exceed the strength of the selected materials.

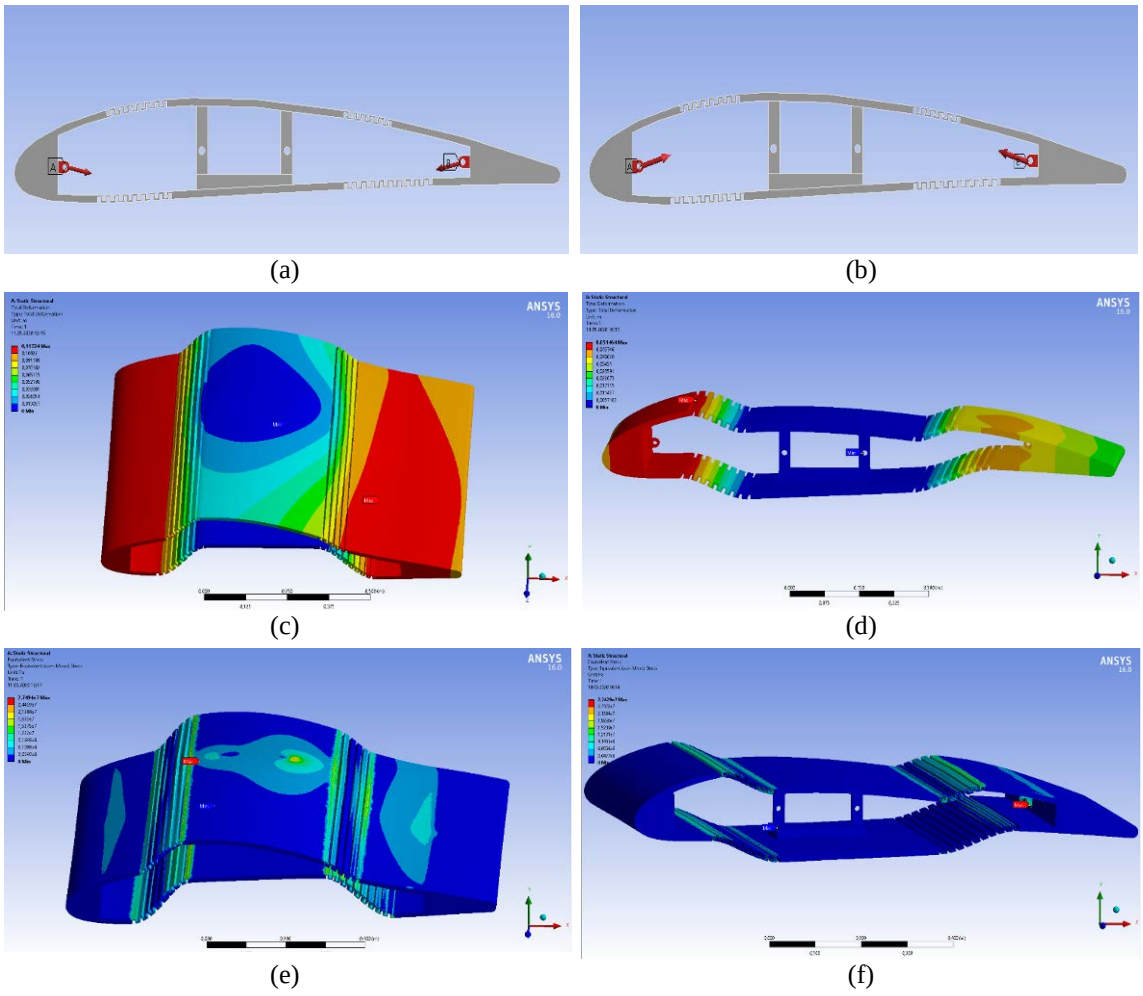

FIG. 4 Finite element analysis of the variable chord morphing wing model: (a) setting the forces for the concave shape of the model, (b) setting the forces for the convex shape of the model, (c) total displacements on the concave model, (d) total displacements on the convex model, (e) equivalent stresses on the concave model, (f) equivalent stresses on the convex model

3.2 Finite element analysis of variable chord morphing wing

For this variable span morphing wing model, a finite element analysis is performed in order to get conclusive results in terms of the displacement of elements at the structure level. Since the model is of such nature, this is the only aspect of interest for this analysis. The studied model had a dimension of 1090 mm along the airfoil chord and a span of 2565 mm.

The meshing of the model (Fig. 5a) was performed with elements of size 10 mm, resulting in a total of 154108 elements joined together by 563808 nodes. The model was fixed to the outer surface of the first rib (Fig. 5b), thus this fastening simulates the embedding of the wing in the fuselage of the aircraft.

The applied force (Fig. 5c) was calculated as the product of: the aircraft load factor (n=3.8), the gravitational acceleration (g=9.81 g/s2), the wing mass (m=92.3 kg) and the safety factor (SF=1.5), and the result is 5161.14 N.

In conclusion, the analysis of the total displacements (Fig. 5d) occurring on the structure of this variable span wing model, showed low values that do not raise problems of such nature that could lead to damage of the structure through reaching a high value of extension.

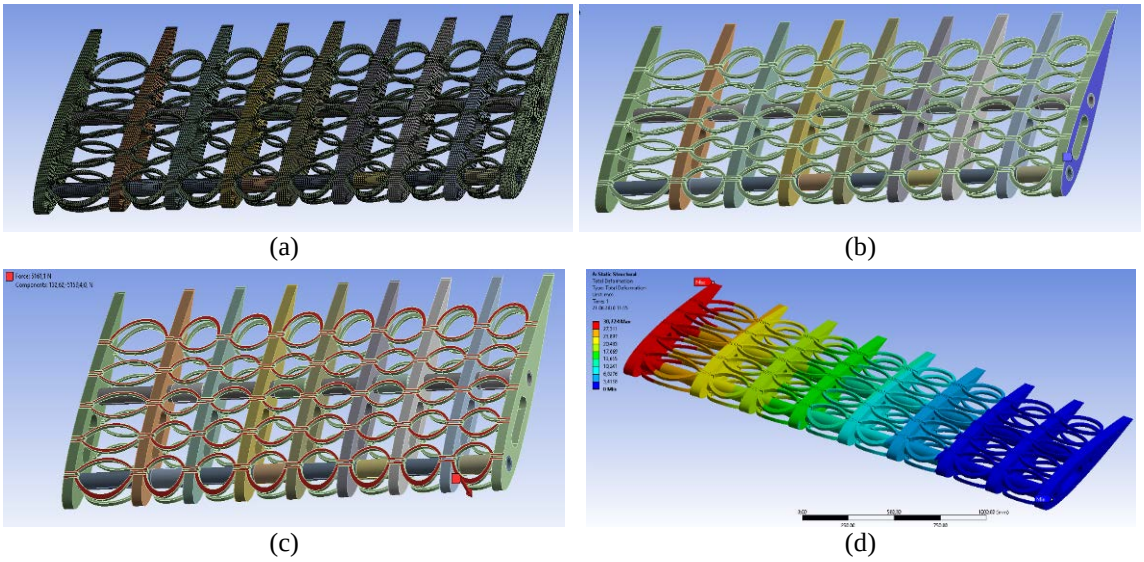

FIG. 5 Finite element analysis of the variable span morphing wing model: (a) model meshing, (b) setting boundary conditions, (c) application of stresses, (d) distribution of total displacements.

4. CFD ANALYSIS OF MORPHING WING MODELS

4.1 CFD analysis of the variable profile morphing wing

In order to carry out the aerodynamic analysis of the designed prototype using the computer-aided fluid dynamics method, the Ansys 16.0 analysis software was chosen. To carry out the CFD analysis, two reference positions where the wing profile of this concept is located were comparatively selected. The first targeted position is the neutral position of the model having as comparison the position of the model with the maximum bending shape obtained in the FEA results. Thus, the second position has a concave shape with a leading edge and trailing edge displacement of about 60 mm from the initial position.

The analysis domain, for the two models (Fig. 6a and Fig. 6b) was created in such a way that in the front of the profile there is a distance 10 times bigger than the chord of the profile, in the upper part of the profile the distance is also 10800 mm, in the lower part the same ratio of 10 times the size of the chord is kept and in the rear part of the profile the distance was set 30 times bigger than the chord. The CFD analyses were carried out for a velocity of 45 m/s, at a standard temperature of 15˚ C and an air density of 1,226 kg/m^3.

Based on the graphical representations (Fig. 6c and Fig. 6d), in both positions of the model it can be observed that the maximum pressure value is at the contact between the fluid and the prototype. If in Fig. 6c a balancing of the pressure with the atmospheric pressure is captured by the green background present in an overwhelming proportion, in Fig. 6d this area is much smaller. This indicates a higher lift force generated.

In the first phase, a rather large red area can be seen on the extrados surface indicating acceleration of the speed on the extrados surface compared to the intrados surface (Fig. 6e and Fig. 6f). At the same time, a reduced area of low velocity surface at the trailing edge can also be observed which represents the generation of low drag. In the second phase, these aspects change, and the velocity acceleration area is dramatically reduced, its

maximum value being repositioned in the leading edge area at the intrados level. On the other hand, the drag generated at the rear of the profile is much higher, an effect developed from the low speeds found at the trailing edge.

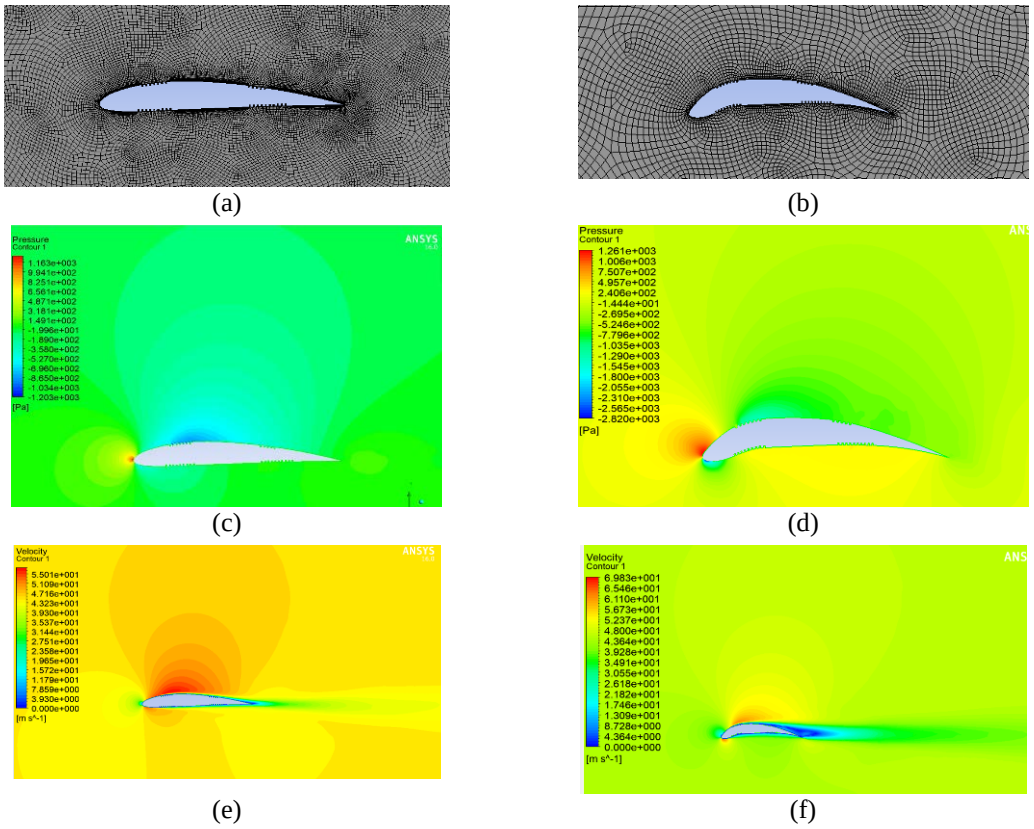

FIG. 6 CFD analysis of variable profile morphing wing: (a) meshing domain – neutral position, (b) meshing domain – deformed position, (c) pressure distribution – neutral position, (d) pressure distribution – deformed position, (e) velocity distribution – neutral position, (f) velocity distribution – deformed position

4.2 CFD analysis of the variable chord morphing wing

The aerodynamic analysis of this morphing wing prototype was carried out using the XFLR5 software system. The modelling of the wing (Fig. 7a) was done from the airfoil and using the 5 displacement positions. The purpose of these analyses (Fig. 7b) is to obtain results on the aerodynamic coefficients (lift coefficient, drag coefficient) of each of the 5 wing displacement positions (position 1 - 2565 mm; position 2 - 2655 mm; position 3 - 2745 mm; position 4 - 2835 mm; position 5 - 2925 mm). From a percentage point of view, taking into account that the wing extension from one stage to the next represents 3.51% of the initial wingspan, the percentage of total displacement amounts to a 14.04% surplus in wingspan compared to the initial position. For the wing analysis settings, a velocity of 45 m/s is entered, and the angle of attack variation was from -5˚ to 15°. This prototype variable span morphing wing offers aerodynamic advantages.

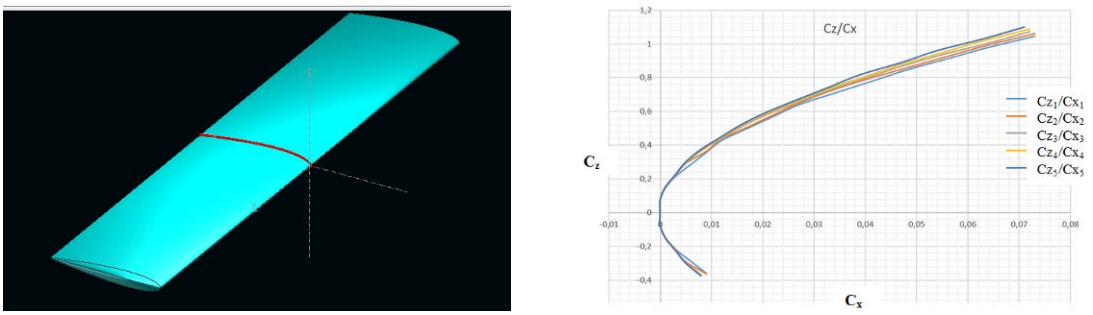

(a) (b)

FIG. 7 CFD analysis of variable chord morphing wing: (a) wing modelling, (b) variation of lift coefficient as function of drag coefficient

5. 3D PRINTING, ASSEMBLY AND OPERATION OF THE VARIABLE PROFILE MORPHING WING

Based on the FEA results, it was concluded that Flexfill 92A is the most suitable material to use to get the desired results. After the CAD model was made, it was saved and inserted into the 3D printing software system. The entire model took 40 hours and 11 minutes to complete and used 45.97 m of filament, with a part mass of 137 g (Fig. 8a). The following elements were used to manufacture the overall assembly: a nano servo controller, servo drive arm, Arduino board, adaptive nano terminal board, 4 sets of connecting wires, battery case holder, linear potentiometer, 2 connecting arms connecting the servo drive arm and the wing model, main wing structure model (Fig. 8b).

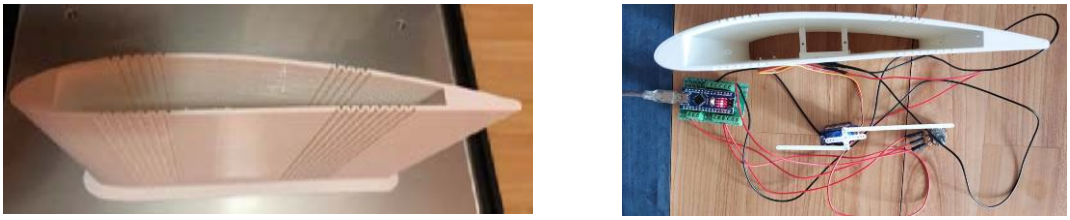

(a) (b)

FIG. 8 Manufacturing and testing of the variable chord morphing wing: (a) 3D printing of the model, (b) physical testing of the variable chord morphing wing.

From a functional point of view, this wing morphing prototype can be divided into two subdivisions. The electrical subdivision where the electrical operation of the digital servo is monitored by means of code inserted on the Arduino board and whose movements are controlled from the potentiometer, and the mechanical subdivision which aims to deform the profile because of the force transmitted from the digital servo arm to the wing itself. The electrical functional subdivision is primarily based on a code which guides the operation of this system. This code is written in Arduino software and is relatively simple. The code is inserted into the Arduino board via a cable. After testing, this system works under normal conditions. In conclusion, this system for modifying the wing to change the geometry is reliable and could be used opted in the near future.

CONCLUSIONS

Over time, due to technological development and highly flexible materials allowing for large elastic deformations, morphing concepts can bring enormous benefits both in terms of aerodynamics, controllability, economics and optimization of the flight itself. In this paper two morphing wing designs have been analyzed which focus on airfoil geometry variation and wing span variation. The structural analyses carried out on the two designs targeted different characteristics. For the airfoil morphing concept, both the equivalent stresses and the total displacements occurring in the model because of a force simulating the deformation caused by the digital servo action were investigated. For the variable span concept, the aspect of additional displacements occurring, both directionally and overall, was closely followed. From an aerodynamic point of view, for the first concept, with variable airfoil, many characteristics of the airflow on the airfoil surface both in the initial position and in a deformed position have resulted which generate a significantly higher lift force. For the second concept, according to the results obtained, it was observed that there is an aerodynamic improvement offered by this prototype. In order to validate these prototypes at the UAV aircraft level, 3D printing can be used as technological developments allow this.

REFERENCES

[1] I. Cîrciu and V. Prisacariu, Command and control of the flying wing in the morphing concept, *Review of the Air Force Academy*, no.1(23), pp. 13-18, 2013;
[2] S. C. Patel, M. Majji, B. S. Koh, J. L. Junkins, O. Rediniotisx, *Morphing wing: A demonstration of aero servo elastic distributed sensing and control*. Tec. report, Texas Institute, 2005;
[3] V. Prisacariu, I. Cîrciu and M. Boşcoianu, Morphing concept of UAVs of the swept flying wing, *Recent Journal*, vol.15, no. 1, pp. 26-33, 2014;
[4] K. Taguchi, K. Fukunishi, S. Takazawa, Y. Sunada, T. Imamura, K. Rinoie, and T. Yokozeki, Experimental study about the deformation and aerodynamic characteristics of the passive morphing airfoil, *Transactions of the Japan Society for Aeronautical and Space Sciences*, vol. 63, no. 1, pp. 18-23, 2020;
[5] C. H. U. Lingling, L. I. Qi, G. U. Feng, D. U. Xintian, H. E. Yuqing, and D. E. N. G. Yangchen, Design, modeling, and control of morphing aircraft: A review, *Chinese Journal of Aeronautics*, vol. 35, no. 5, pp. 220-246, 2022;
[6] D. W. Martinez, M. T. Espino, H. M. Cascolan, J. L. Crisostomo, and J. R. C. Dizon, A comprehensive review on the application of 3D printing in the aerospace industry, *Key engineering materials*, vol. 913, pp. 27-34, 2022;
[7] S. Singamneni, L. V. Yifan, A. Hewitt, R. Chalk, W. Thomas and D. Jordison, Additive manufacturing for the aircraft industry: a review, *Journal of Aeronautics & Aerospace Engineering*, vol. 8, no. 1, pp. 351-371, 2019;
[8] A.O. MohamedZain, H. Chua, K. Yap, P. Uthayasurian and T. Jiehan, Novel Drone Design Using an Optimization Software with 3D Model, Simulation, and Fabrication in Drone Systems Research, *Drones*, vol. 6, 2022;
[9] D. A. Popica and S. M. Zaharia, Design, aerodynamic analysis and additive manufacturing of a radio-controlled airplane, *Journal of Industrial Design and Engineering Graphics*, vol. 18, no. 1, pp. 39-44, 2023;
[10] A.E. Rivero, S. Fournier, R.M. Heeb and B.K.S. Woods, Design, Manufacture and Wind Tunnel Test of a Modular FishBAC Wing with Novel 3D Printed Skins, *Applied Sciences*, vol. 12, 2022;
[11] M. S. Parancheerivilakkathil, R. M. Ajaj and K.A. Khan, A compliant polymorphing wing for small UAVs. *Chinese Journal of Aeronautics*, vol. 33, pp. 2575–2588, 2020;
[12] T. Mkhoyan, N. R. Thakrar, R. De Breuker and J. Sodja, Morphing wing design using integrated and distributed trailing edge morphing, *Smart Materials and Structures*, vol. 31, no. 12, pp.125025 - 125045, 2022;
[13] F. Previtali, R. Bleischwitz, A. Hasse, L. F. Campanile and P. Ermanni, *Compliant morphing wing*, pp. 1–13, 22nd International Conference on Adaptive Structures and Technologies, Greece, Corfu, October 10-12, 2011;

[14] W. Johannisson, R. Harnden, D. Zenkert and G. Lindbergh, Shape-morphing carbon fiber composite using electrochemical actuation. *Proceedings of the National Academy of Sciences*, vol. 117, no. 14, pp. 7658-7664, 2020;

[15] S. M. Afonin, Structural diagram of actuator for nanobiotechnology, *Journal of Biogeneric Science and Research*, vol. 7, no. 4, pp. 1-6, 2021;

[16] M. T. Kammegne, R. M. Botez, L. T. Grigorie, M. Mamou and Y. Mébarki, A new hybrid control methodology for a morphing aircraft wing-tip actuation mechanism, *The Aeronautical Journal*, vol. 123, no. 1269, pp. 1757-1787, 2019.

[17] V. Brailovski, P. Terriault, T. Georges and D. Coutu, SMA actuators for morphing wings, *Physics Procedia*, vol. 10, pp. 197-203, 2010;

DESIGN AND ANALYSIS OF A 3D PRINTED RC AIRCRAFT

Paul-Sebastian SUCIU
"Transilvania" University of Braşov, Romania (paul.suciu@student.unitbv.ro)

Sebastian-Marian ZAHARIA
"Transilvania" University of Braşov, Romania (zaharia_sebastian@unitbv.ro)
ORCID: 0000-0002-8636-5558

DOI: 10.19062/1842-9238.2023.21.1.2

Abstract: *3D printing of radio-controlled aircraft brings a major advantage, especially for prototype aircraft, as it can provide performance information in the shortest time and at the lowest cost. In this study, a model of a radio-controlled aircraft with high wing and tricycle landing gear was designed, aerodynamically analysed, simulated in FEA and manufactured by 3D printing. The aerodynamic performance showed a lift coefficient of 1.15 at a drag coefficient value of 0.10. From the FEA simulation, the wing structure was proven to withstand the stresses arising during the flight of the radio-controlled aircraft. It also demonstrated the feasibility of 3D printing in the case of radio-controlled aircraft prototypes, ready for the first flight tests.*

Keywords: *3D printing, radio-controlled aircraft, CFD analysis, finite elements analysis*

1. INTRODUCTION

There is a vast diversity of radio-controlled aircraft (or simple models) that can be produced by 3D printing, the deciding factor being the flight mission. In terms of design, there are small-scale, semi-scaled or prototype models. Small-scale and semi-scaled models are reproductions of existing aircraft, the only difference being the degree of accuracy; prototypes do not follow the design of an existing aircraft [1], but rather the development and testing of the innovative aircraft model [2].

Several types of radio-controlled aircraft that have been manufactured by 3D printing are presented below:

• Training aircraft are made for beginners to learn to fly. They have a conventional design, with the wing placed above the fuselage to ensure maximum stability. Training aircraft can be powered by electric motors or internal combustion motors. Their range is vast and represents a large subdivision of RC models [3].

• Sport aircraft can be designed as the next step after the pilot's becoming familiar with a training aircraft, but there is also the option of using them for the same purpose. Sport aircraft have a higher aerobatic capability than training aircraft. This is made possible by placing the wing at the middle or under the fuselage [4].

• The hydroplanes are a less popular choice because of the need for a landing site (preferably a lake). As with aerobatic aircraft, these types of RC models require a higher degree of experience, especially when it comes to landings [5].

• Warbird type of aircraft have always been a popular choice for RC models; the aesthetic design and good aerodynamic characteristics have made this type one of the most popular.

The term 'Warbird' refers to fighter aircraft from the time of the World War I and particularly the World War II. The P-51 Mustang, Spitfire and Corsair F4U are some classic examples. This range is not necessarily suitable for beginners, but there are 'Warbird' type models designed for this purpose [6].

- Aerobatic planes are specifically designed to perform aerobatics. This type of aircraft typically has oversized control surfaces and motor, and a mid-wing. This category is addressed to people with a certain degree of experience [7].

Based on the analysis of the current state of knowledge, the following aspects can be concluded [8-10]: 3D printing can be used to manufacture various aircraft prototypes in a relatively short time, without the need for a mould; additive technology has the potential to replace a multitude of current technologies; the most widely used material for 3D printing of models is polylactic acid (PLA), the wingspan of the aircraft varies between 900-16000 mm, the models have a relatively high mass, in the case of 3D printers intended for the general public, their accuracy is low.

2. RC MODEL DESIGN

Based on the analysis of the structural solutions, the design of a training aircraft was chosen with the following structural details: the wing has a rectangular shape and is placed above the fuselage; the fuselage is cylindrical; the shape of the horizontal empennage is trapezoidal; the empennages are arranged in a conventional configuration; the landing gear is of the tricycle type with tail wheel. The software system used for the wing design, and therefore for the design of the whole aircraft, was SolidWorks 2019. Next, the steps of the wing design are summarized: the airfoil (Clark Y) was inserted, the ribs were created (Fig. 1a), the ribs were cut for the lightening holes, the servo mount was set (Fig. 1b).

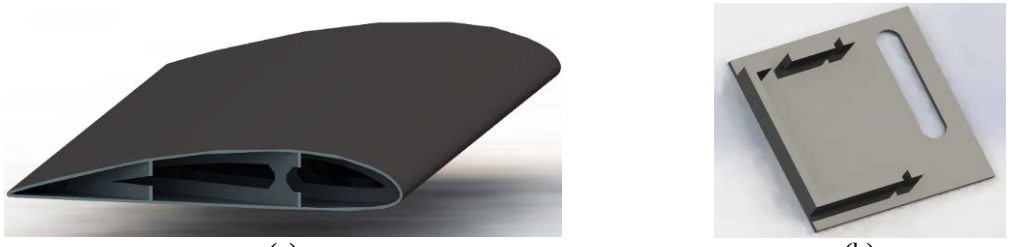

(a) (b)

FIG. 1 Three-dimensional model of the RC aircraft wing: (a) wing rib structure, (b) servo mount.

The profile chosen for the horizontal (Fig. 2a) and vertical (Fig. 2b) empennage was NACA 0009. The ribs for the two empennages have been designed as for the wing.

(a) (b)

FIG. 2 Three-dimensional model: (a) horizontal empennage, (b) vertical empennage.

In order to design the fuselage, planes and circular sections were created and then the assembly areas of the wing and motor mount were cut out (Fig. 3a). The 3D model of the radio-controlled aircraft prepared for 3D printing is shown in Fig. 3b. The 3D model (Fig. 3b) had the following dimensions: wingspan 900 mm, length 675 mm and height 180 mm.

(a) (b)

FIG. 3 RC aircraft design: (a) structure of the fuselage, (b) final model of the RC aircraft.

3. CFD ANALYSIS OF 3D PRINTED RC AIRCRAFT

The software system used for the CFD analysis of the radio-controlled aircraft was XFLR5 V6.48. In order to obtain the wing and aircraft curve polars, it is necessary to analyse in advance the profiles used (Clark Y and NACA 0009). For the wing analysis, the following input data were established: default speed of 13.8 m/s; the angles of attack for which this analysis is performed range from - 5° to 12°.

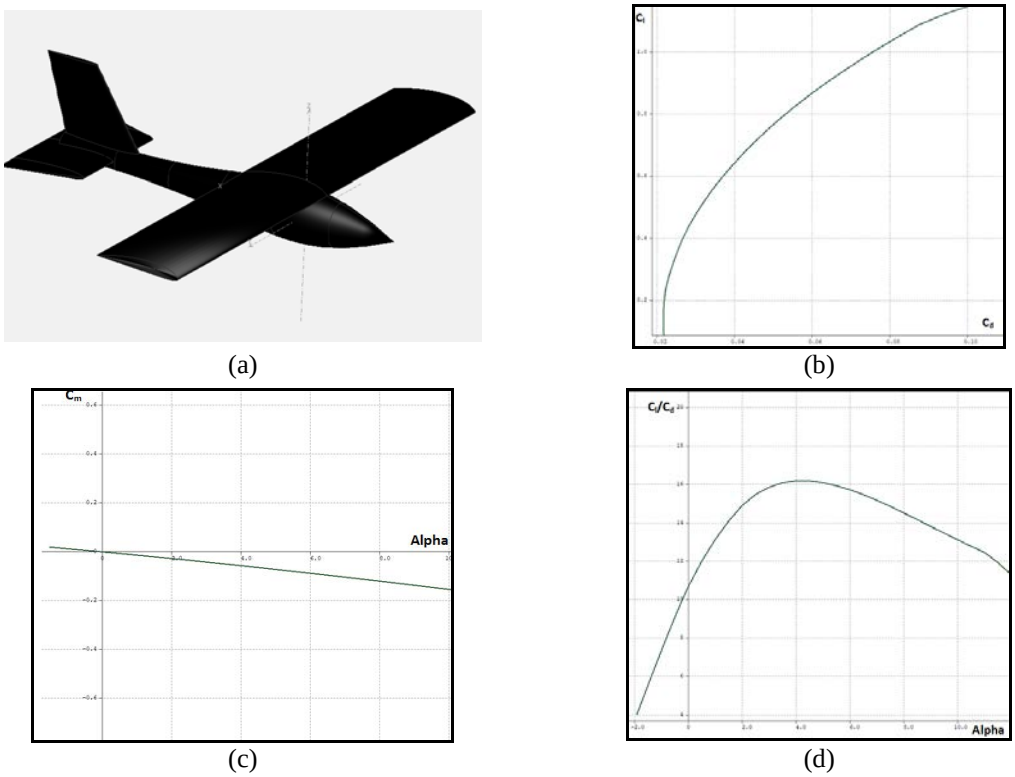

(a) (b)

(c) (d)

FIG. 4 The preliminary aerodynamic analysis of the RC airplane: (a) 3d model of the aircraft, (b) variation of lift coefficient as function of drag coefficient, (c) variation of moment coefficient as function of the angle of attack, (d) variation of lift/drag ratio as function of the angle of attack.

After 3D modelling of the entire aircraft (Fig. 4a) the most important results of the aerodynamic analysis were determined: variation of lift coefficient as function of drag coefficient (Fig. 4b), variation of moment coefficient as function of angle of attack (Fig. 4c), variation of lift/drag ratio as function of angle of attack (Fig. 4d). The maximum value of the lift coefficient was 1.15 units for a value of drag equal to 0.103 units (Fig. 4b). To have a statically stable aircraft, the slope of the Cm- Alpha curve (α) must be negative. The smaller the slope value, the more stable the aircraft, so it can be seen in Fig. 4c that the slope value is negative. The lift/drag ratio of the aircraft increases with increasing the angle of attack. It reaches a maximum value of 16 units at 4° angle of attack. After exceeding this angle, the fineness decreases (Fig. 4d).

4. FINITE ELEMENT ANALYSIS OF THE 3D PRINTED RC WING

The finite element analysis of the strength structure is carried out for the wing semispan in the Ansys 2016 software system. The semispan was chosen to simplify the fixing method. The force applied for the wing stress was 29.43N, calculated as the product of the load factor (n=2), the aircraft mass (m=1 kg), the safety factor (SF=1.5) and the gravitational acceleration (9.81 m/s^2). Next, some important aspects were established: the material used for the model, in this case polylactic acid, was defined, the mashing of the model was performed with an element size of 3 mm, the wing was fixed in the embedding area and the force was uniformly applied over the entire surface of the shell (F=29.43N). The total displacements showed a maximum of 6.06 mm in the tip area of the wing (Fig. 5a). The maximum equivalent stresses (Fig. 5b) had values of 5.64 MPa near the embedment area of the wing to the fuselage. It can be concluded that the equivalent stress does not exceed the compressive strength of the PLA material. The maximum compressive strength of polylactic acid is 60.5 MPa, so the wing withstands the applied loadings.

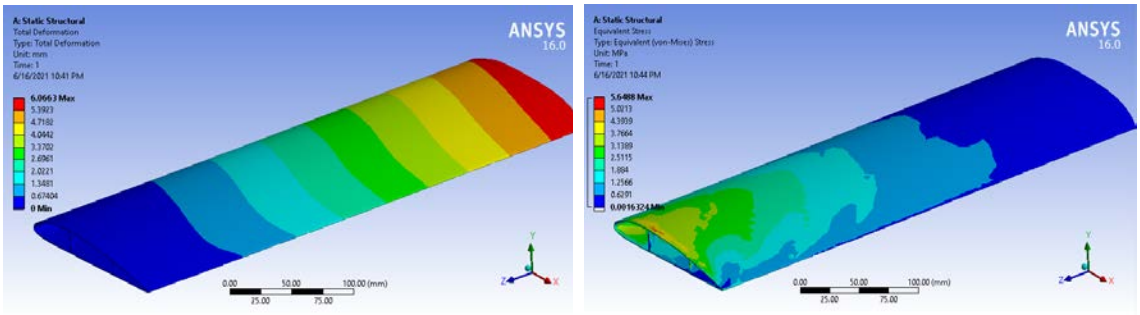

(a) (b)

FIG. 5 Finite element analysis: (a) total deformation, (b) equivalent stress.

5. MANUFACTURING THE RADIO-CONTROLLED AIRCRAFT PARTS USING 3D PRINTING

The 3D printer used to manufacture the radio-controlled aircraft parts was the Zortrax M200 Plus. The software system used to 3D print the aircraft parts was Z-Suite. Among the most important parameters we can list: the thickness of the deposition layer was 0.14 mm and the infill density was 50%, the printing temperature was 200 °C, the temperature of the bed plate was 30°C, and the material was polylactic acid (PLA). Figure 6a shows some of the parts prepared for 3D printing in the Z-Suite software system and Fig. 6b shows the 3D printed parts.

Also, in Fig. 6c some sections of the fuselage were prepared for 3D printing and in Fig. 6d these parts can be seen after they were printed. The total printing time for all the parts of the aircraft was 171 hours and the amount of PLA filament required was 1270 grams.

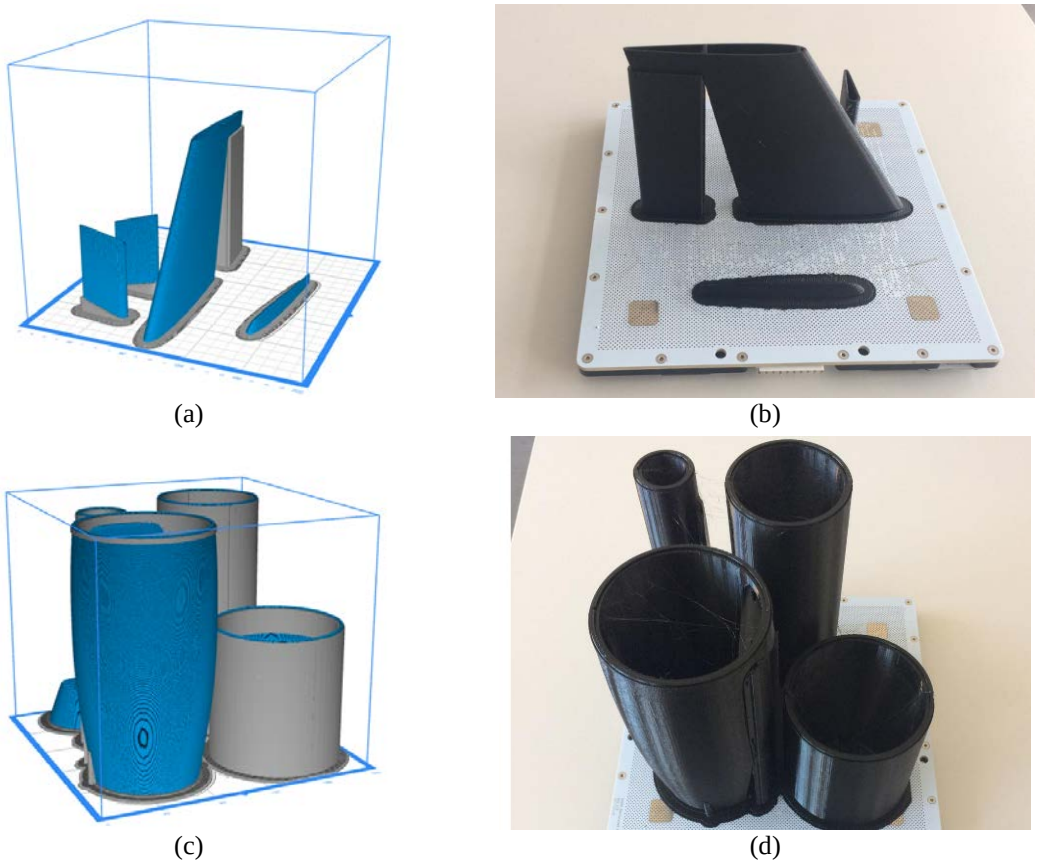

(a) (b) (c) (d)

FIG. 6 Steps in the 3D printing process: (a) preparation for manufacturing of the vertical fuselage, (b) 3D printed vertical fuselage, (c) preparation for manufacturing of the fuselage sections, (d) 3D printed fuselage sections.

6. ASSEMBLY AND GROUND TESTING OF THE 3D PRINTED RC WING

To assemble the aircraft, a series of steps were carried out: the support material from the 3D-printed parts was removed, the rear sub-assembly consisting of the empennages and the last fuselage section was glued (Fig. 7a); the parts of the aircraft were sanded with sandpaper, the wing sections were glued (Fig. 7b) and two-component adhesive was used to make all the joints; before gluing the wing tips, the servo extensions were inserted; for aesthetic reasons, the radio-controlled aircraft was painted; the next step involved attaching the control surfaces using a fibreglass adhesive strip; the servo-mechanisms were assembled and coupled to the control rods.

Regarding the manufacturing and assembly of the landing gear (Fig. 7c), it was decided to use stainless steel rods (D=2 mm). The landing gear was arc welded at the wheels. The mounting of the rear landing gear was done by means of pocket hole screws. The next step was the assembly of the electrical parts consisting of the regulator, transmitter, battery and propeller. The parts are fixed inside the fuselage by means of an adhesive strip with Velcro, except for the motor, which is fixed to the motor mount with screws.

The electrical parts used were brushless outrunner motor SUNNYSKY X2212, the speed controller used is brushless Fly Pro - 40A, LiPo battery 2700 mAh, the transmitter and receiver used to fly the aircraft are the Radiolink AT9S. The final design of the aircraft is shown in Fig. 7d.

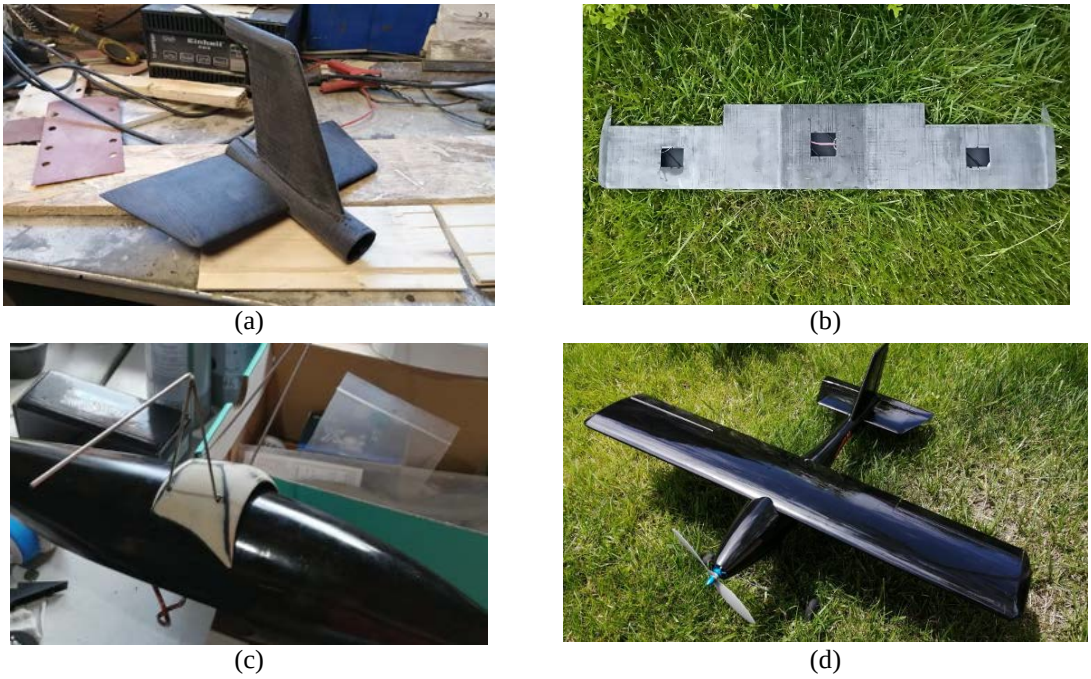

(a) (b) (c) (d)

FIG. 7 Stages in the assembly process: (a) gluing the rear subassembly, (b) assembling and gluing the wing, (c) manufacturing the landing gear, (d) the 3D printed radio-controlled aircraft.

In the last stage, ground testing of the control surfaces was carried out as follows: rudder deflection (Fig. 8a), elevator deflection (Fig. 8b), aileron deflection and the correct operation of the electric motor was also checked (Fig. 8c).

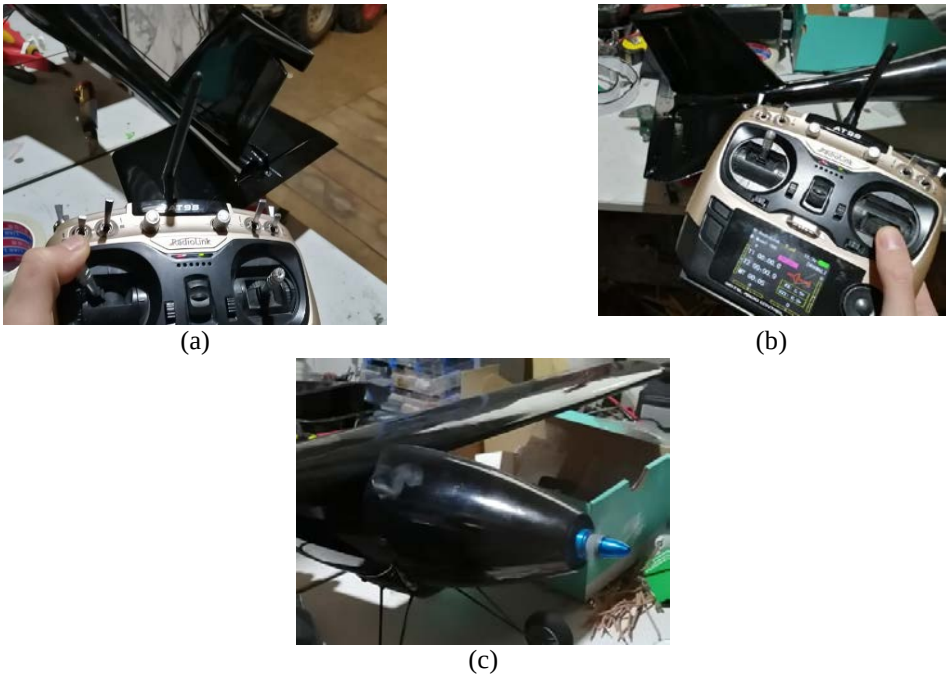

(a) (b) (c)

FIG. 8 Ground testing: (a) motor testing, (b) rudder movement, (c) elevator deflection.

CONCLUSIONS

The current state of knowledge about aircraft shows the simplicity of additive processes, in that no moulds are required to make the models. Another advantage worth mentioning in this context is the reduced manufacturing time. The designed and 3D printed aircraft has a mass of about 1800 g and a range of 6-10 minutes, depending on the type of flight. From the CFD analysis the polar curves of the most important aerodynamic coefficients (lift coefficient, drag coefficient and momentum coefficient) were determined and plotted. From the FEA simulation, the maximum compressive strength of polylactic acid is much higher compared to the equivalent stress obtained from the finite element analysis of the wing. The 3D printing of the radio-controlled aircraft parts from PLA filament was carried out without any problems and the manufacturing time was 171 hours.

The main goals of the assembly technology were to manufacture a visually aesthetic and structurally strong aircraft. In the final phase, ground tests were carried out to check the operation of the control surfaces and the electric motor. In conclusion, it is possible to manufacture aircraft using 3D printing in a relatively short time and without the need for moulds, at low cost, using an affordable additive process.

REFERENCES

[1] A. Olejnik, S. Kachel, R. Rogólski and J. Milczarczyk, The concept and methodical assumptions for the development of dynamically scaled aircraft model (passenger aircraft), MATEC Web of Conferences, vol. 304, 2019;

[2] K. Patel, Y. Parmar, V. Parmar, H. Mistry and M. Tandel, A Review Article on Design and Development of Radio-Controlled Airplane, International Journal of Advances in Engineering and Management, vol. 2, no. 7, pp. 41-46, 2008, 2019;

[3] *** 3D LabPrint, QTRAINER aircraft. Available at https://3dlabprint.com/shop/qtrainer/, accessed on 10 May 2023;

[4] D. A. Popica and S. M. Zaharia, Design, aerodynamic analysis and additive manufacturing of a radio-controlled airplane, Journal of Industrial Design and Engineering Graphics, vol. 18, no.1, pp.39-44, 2023;

[5] *** RC3DPRINT, Grumman Mallard aircraft. Available at https://www.rc3dprint.com/mallard, accessed on 12 May 2023;

[6] *** 3D LabPrint, P51-D MUSTANG aircraft. Available at https://3dlabprint.com/shop/p51-d-mustang/, accessed on 11 May 2023;

[7] *** PLANEPRINT, SHARD aircraft. Available at https://www.planeprint.com/shard, accessed on 11 May 2023;

[8] I. S. Pascariu and S. M. Zaharia, Design and testing of an unmanned aerial vehicle manufactured by fused deposition modeling, *Journal of Aerospace Engineering*, vol. 33, no. 4, 2020;

[9] I. Skawiński and T. Goetzendorf-Grabowski. 2019. “FDM 3D printing method utility assessment in small RC aircraft design.” Aircraft Eng. Aerosp. Technol. 91 (6): 865–872;

[10] M., Hassanalian and A. Abdelkefi, Classifications, applications, and design challenges of drones: A review, *Progress in Aerospace Sciences*, vol. 91, pp. 99-131, 2017.

ASPECTS RELATED TO THE VERSATILITY OF THE F-16 MLU AIRCRAFT

Ionică CÎRCIU
"Henri Coanda" Air Force Academy, Brașov, Romania (circiuionica@yahoo.co.uk)
ORCID: 0000-0002-3781-4687

DOI: 10.19062/1842-9238.2023.21.1.3

Abstract*: The intelligent use of the armament capabilities of the modernized F16 aerial platform, combined with the gradual training of the pilots, gives Romania a plus in the fulfillment of the missions assigned to the Air Force. Increasing the number of F16 aircraft from 17 to 49, diversifying armament capacities, training aeronautical personnel and the sustained, pragmatic use of these resources for a few years is bound to enable the Romanian Air Force to gradually advance towards higher generation aircraft.*

Keywords: *agility, variants of armament, transition period, engagement.*

1. INTRODUCTION

The strategy of modernizing Romania's combat aircraft fleet, as observed, broadly included the stages: the first is represented by the staggered purchase of 17 F-16 aircraft to equip a squadron (Portugal) in conjunction with the training of aeronautical personnel and the preparation of the infrastructure for the new technique; the second stage consisted in the introduction into combat service of the F16 plane in parallel with the MiG-21 plane (which was gradually abandoned); a third stage is the addition of 32 F16 aircraft (Norway), in order to obtain a consistent vertical combat component, the numerical capacity reaching 49 F16 aircraft corresponding to three squadrons that will ensure the missions of the air forces, especially those of the air police and the last stage will be reached by equipping the F-35 aircraft around 2030 according to the CSAT decision, at which time the F-16s will be gradually withdrawn from operation [1]. Returning to the current context, the 32 aircraft purchased from Norway are in the M 6.5.2 configuration, superior to the 17 aircraft in the M 5.2 R configuration [1,2].

The 49 Romanian aircraft will gradually be upgraded to AEROSTAR in a superior M. 6. X configuration, according to the Romanian Ministry of Defence [2].

2. THE VERSATILITY OF THE F-16 AIRCRAFT AND ALTERNATIVE ROLES

The essential added value of the F-16 plane is its versatility. The aircraft, designed as a light supersonic combat aircraft, can be armed with a wide range of weapons, such as air-to-air missiles of the latest generation, with increased accuracy and range, with high jamming protection, bombs and intelligent guided or classic munitions.

The ability to use of active electronic countermeasures to avoid enemy radars or passive radars such as electromagnetic dipoles or thermal traps should not be omitted either.

The F-16 is equipped with advanced optoelectronic sensors, including a multimode radar system that provides an unprecedented level of situational awareness.

An important sensor for the destruction of ground or aerial targets is the versatile and advanced AN/APG-66(V)2 radar, with good capabilities for searching, tracking and framing targets in multiple scenarios.

The AN/APG-66(V)2 radar is the main sensor for both air-to-air and air-to-ground targets, providing the pilot with information on the combat situation and possibilities for target identification [3,4,5].

The AN/APG-66(V)2 on-board radar has multiple operating modes, allowing the *F-16A/B MLU Block 15* to adapt to various mission situations. Some of its key roles are:

1. Air-to-air interception modes:

a. Track While Scan (TWS): In this situation, the radar can simultaneously track multiple aerial targets while scanning the airspace for additional threats [4].

b. Range While Search (RWS): RWS mode allows scanning over a wide area for possible targets with ranging to them [5].

c. Single Target Track (STT): when the radar locks on a target. This mode provides precise target tracking, allowing the aircraft to hit the selected enemy with precision-guided munitions [3,4,5].

2. Air-to-ground interception [3,4,5] :

a. GroundMoving Target Indication (GMTI): GMTI mode allows the radar to detect and track moving ground targets, even in crowded environments [4].

b. SyntheticAperture Radar (SAR): by using SAR technology, the radar can form high-resolution radar images of the Earth's surface, enabling accurate target identification [4].

In essence, the presented radar is capable and adaptable, leading to a significant increase in the combat capability of the F-16. We can point out as a plus of this radar: advanced features that allow the activation of last-generation missiles, multiple operating modes and increased resistance to jamming, which makes the F-16A/B MLU Block 15 a feared multi-role fighter. As a minus we can point to the fact that a radar with a larger range of action would be required [3,4,5].

3. SOME OF THE ADVANCED WEAPONS OF THE F-16 MLU AIRCRAFT

Among the on-board weapons of the F 16 A/B MLU, we mention:

1) *Air-to-air missiles*:

- AIM-9 Sidewinder, short-range missile, self-guided in infrared, fig.1 [5].

The missile used mainly on aerial targets, has good maneuverability with the possibility of tracking targets from various angles, increased resistance to jamming.

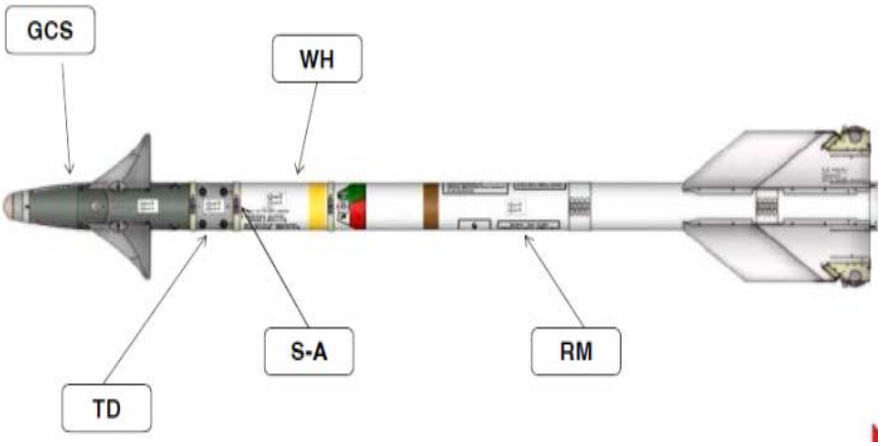

FIG.1 AIM-9 Sidewinder [5]

The rocket is composed of five major sections: 1. Guidance Control Section (GCS) 2.Target Detector (TD) 3.Safety arming device (S-A) 4. Focos (WH) 5. Rocket motor (RM) [5,6].

-AIM-120 AMRAAM, medium-range missile, with active radar type action principle.

The rocket is part of the range of weapons dedicated to aerial supremacy, used mainly on aerial targets, it has its own radar-type guidance system with high target tracking accuracy and good jamming protection [6].

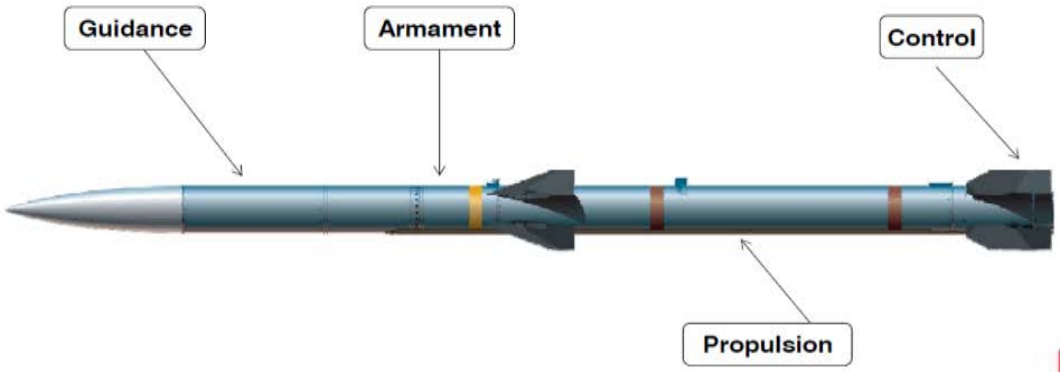

FIG.2 AIM-120 AMRAAM [6]

Below, we have illustrated an arming option using the two types of missiles in a possible air interdiction mission:

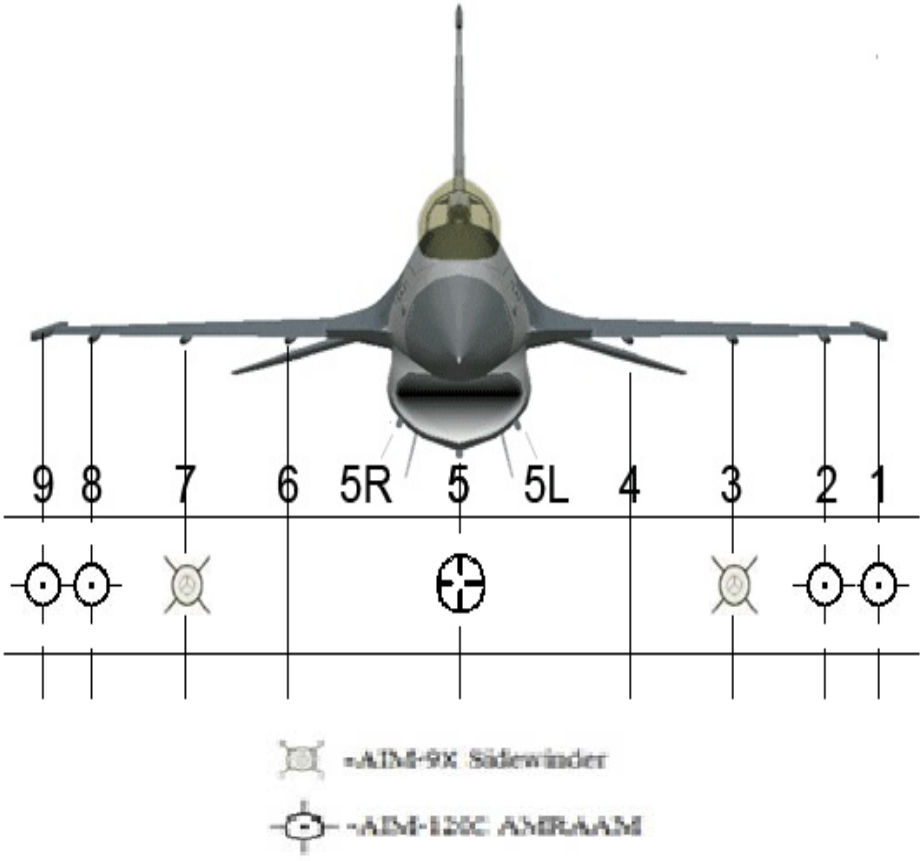

FIG.3 Configuration of the ground attack variant [6.7]

2) *Air-to-ground weapons*:

– Air-to-ground missile/AGM-65 Maverick, which relies on 3 types of sensors: infrared, laser and video camera. The composition of the rocket is modular, which allows it to be assembled in various configurations, depending on the mission. The missile has an increased striking power against a multitude of types of armored or unarmored, tactical, air defense targets, ships, mobile transport systems, warehouses, communication points or troop management [7].

FIG. 4 AGM-65 Maverick [7]

The F-16 MLU allows for the integration of new advanced weapons systems, which leads to the permanent increase of the aircraft's capacity, as well as to a higher efficiency in combating threats and increased versatility, allowing for the increase of omni-role functions. This integration enables precise targeting, a wider range of weapon selections and threat engagement methods in both air-to-air and air-to-surface situations.

We consider the following possibilities:

The maximum efficiency (E) is considered as the sum of the proposed targets ($\sum_{i=1}^{n} n_i$) that must be hit and the destruction power (Ω_i), corroborated by the exits of the aircraft ($\sum_{j=1}^{n} i_j$) multiplied by the number of aircraft per exit (M) [8]:

$$\Omega_i = \frac{\sum_{k=1}^{n} p_k}{N} \quad [8] \tag{1}$$

Where

$$E = \frac{\sum_{i=1}^{n} n_i + \Omega_i}{\sum_{j=1}^{n} i_j \bullet M} \quad [8] \tag{2}$$

$\sum_{k=1}^{n} p_k$ is the total number of attacks/objectives required to eliminate the chosen targets – the number of objectives [8] .

We have:

3 targets, 6 F-16 aircraft scheduled in 3 departures of 2 aircraft each.

The following armament is used: AGM-65 H.

$$\Omega_i = \frac{10}{3} = 3{,}33$$

$$E_M = \frac{\sum_{i=1}^{n} n_i + \Omega_i}{\sum_{j=1}^{n} i_j \bullet M} = \frac{6{,}33}{9} = 70\%$$

The acceptable yield of 70% is therefore 2 hits for the first target, 3 for the second target, 5 for the third (and a total of 10).

4. CONCLUSIONS

Permanently sustained efforts to implement advanced weapons technologies such as missiles and guided bombs with improved precision and increased jamming protection are recommended.

As the missions may vary according to the new situations and requirements, it is recommended to ensure increased flexibility and adaptability in the sense of diversifying the armament of aircraft equipped with intelligent ammunition and with a wider effective range of action.

REFERENCES

[1] *** Defense Romania Team / 11 aprilie 2023;
[2] *** Cer Senin –Revista Forţelor Aeriene, *Programul Avion Multirol - o nouă etapă*, 2015;
[3] P. F. Goree, *F-16 APG-66 Fire Control Radar Case Study Report (IDA/OSD R&M) (*Institute for Defense Analyses/Office of the Secretary of Defense Reliability and Maintainability Study*);*
[4] L. Kuchinski and T. Patton, *The APG-66 radar and its derivative applications*, https://doi.org/10.2514/6.1984-2609;
[5] https://www.f-16.net/f-16_armament.html;
[6] *** http://www.f-16.net/f-16_*versions_article* 9.html.;
[8] *AGM-65 Maverick Tactical Air-Ground Missile, United States of America. Airforce Technology.com. Archived* from the original on 22 July 2015. *Retrieved 17 July 2015*;
[9] Gh. Constantinescu, *Bazele şi construcţiei sistemelor de armament*, Ed.ATM Bucuresti, 1994.

QUALITY OF SERVICE AND SECURITY OF AERONAUTICAL COMMUNICATION NETWORKS

Ovidiu PĂSCUȚOIU
"Henri Coandă"Air Force Academy, Brașov, Romania (ovidiu.pascutoiu@afahc.ro)
ORCID: 0009-0009-6918-0218

Maria-Daniela UNGUREANU
University "Politehnica" of Bucharest, Romania (danielatache26@yahoo.com)

DOI: 10.19062/1842-9238.2023.21.1.4

Abstract: *Aeronautical communication networks play a decisive role in the aviation industry, enabling real-time data exchange between various systems such ground stations, air traffic control and aircraft. Making sure that both requirements – high-quality-service and security – are met is mandatory to guarantee the efficiency, safety and reliability of aeronautical operations. This paper will go through a comprehensive inquiry of the quality of service and security of aeronautical communication and the relationship between them. The main focus of this paper is the security of aeronautical communications. The paper will examine the main types of aircraft communication types and will describe the cyber threats and the security measures applicable in order to mitigate the threats accordingly.*

Keywords: *communication, security, quality, service, encryption, digital, standard*

1. INTRODUCTION

Just like most industries, the aviation industry continues to embrace digitalization, therefore it is clear that aeronautical communications have become a critical concern.

There are many types of aeronautical communication networks, demonstrating how the digital era landscape has constantly evolved during the last 50 years.

Each type of aeronautical communication has its own particularities in terms of quality of service, performance and security.

This article will emphasize the quality of service and security of the main types of aeronautical communication, communication which is such a compulsory asset in order to properly carry out aviation operations.

The quality of service and aviation security are two different requirements; thus, they should be handled by means of different approaches, and with different objectives in mind. Of course, some QoS measure could alter security and vice versa, but this does not necessary mean that the two requirements are mutually exclusive.

Regardless of the type of communication considered (air to air communication/AAC or ground-based communication), security must be addressed and maintained properly in order to ensure the safety of aviation missions.

The paper is therefore composed of four parts:

- The types of aeronautical communications;
- Various QoS parameters for each type of communication;
- Specific cyber threats for these types of network communications;
- Security measures and solutions.

2. TYPES OF AERONAUTICAL COMMUNICATIONS

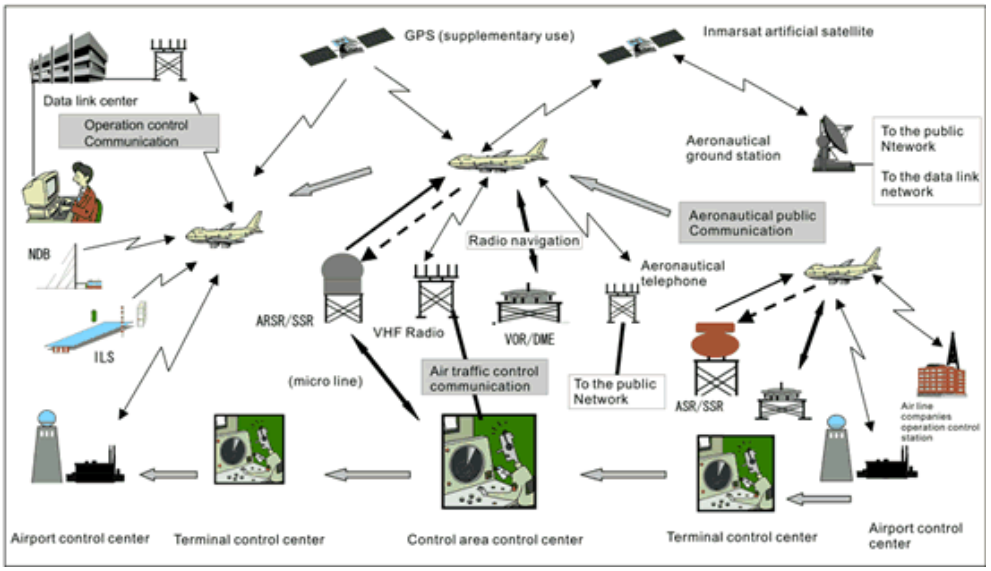

FIG. 1 Types of aeronautical communications

As shown in the image above, aeronautical communication involves many types of communication, whether we are talking about air to ground communication or air to air data transmission.

The types of aeronautical communications can be classified as follows:

- **Analog** communications;
- **Digital** communications;
- **Radio Frequency Identification**;
- **Positioning** systems.

Analog communications can be divided into:

- Very High Frequency Voice Communication (**VHF**);
- High-Frequency Voice Communication (**HF**);
- Emergency Locator Transmitter (**ELT**);
- Navigational Aids.

Example of digital communication include:

- **VHF** Data Link;
- **VoIP** communication;
- **Satellite** communication;
- **Controller-Pilot** Data Link Communication system;
- Aircraft Communications Addressing and Reporting System (**ACARS**);
- Automatic Dependent Surveillance-Broadcast (**ADS-B**).

RFID systems can be divided into:

- **Active** RFID;
- **Semi-active** RFID;
- **Passive** (Battery-Assisted) RFID;
- Near Field Communication (**NFC**).

Positioning systems can be set up as:

- Global Navigation Satellite System (**GNSS**);
- Distance Measuring Equipment (**DME**);
- Tactical Air Navigation (**TACAN**);
- Microwave Landing System (**MLS**).

3. QUALITY OF SERVICE

In order to properly analyze the types of aeronautical communication, we will draw a comparison based on the criterion of the quality of service, as follows:

Table 1 – Quality of service parameters for different types of aircraft communication

Type of communication	Analog	Digital	RFID	Positioning systems
Latency	Variable	Low latency	Depending on read range and accuracy	Low latency
Reliability	Variable	Highly reliable	Reliable	Reliable
Availability	Line-of-sight based	Bandwidth dependent	High availability	Very high availability
Coverage	Ground-based transmitters	High coverage	Anti-collision algorithms based	Very high coverage
Interference	Susceptible to interference	Low interference	Susceptible to interference	Very low interference
Audio quality	Noise reduction	High quality	N/A	N/A
Integration with other systems	No	Interoperability with other communication systems	Allow integration but not a main concern	Yes
Security	Low security / No security	High concern	Vital	High concern
Frequency management	Important	Critical	Essential	N/A

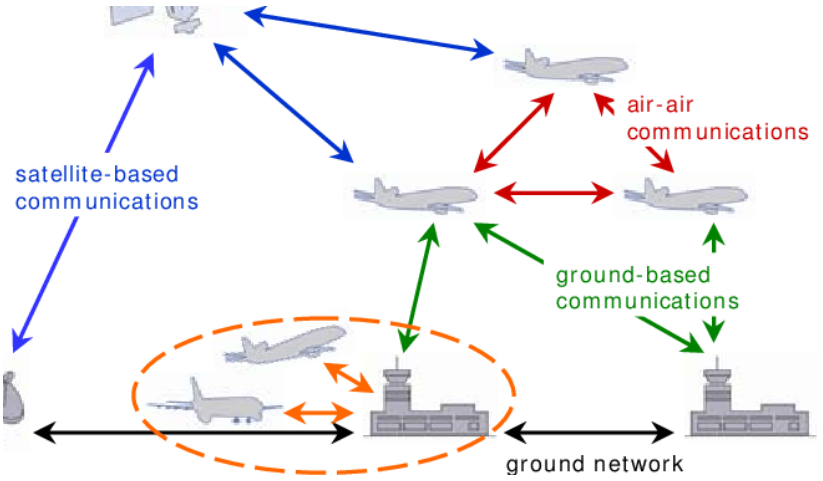

FIG. 2 Aeronautical communication

4. CYBER-THREAT LANDSCAPE

There are many challenges regarding aviation security. Some examples include but not limited to:

- Signal interference;
- Limited bandwidth;
- Unsecure channels;
- Lack of security awareness.

These vulnerabilities can lead to potential damage depending on the attack vector and the surface area.

Table 2 – Main cyber threats-attack vector-damage in aviation communications

Cyber threat	Attack vector	Potential damage
Unauthorized access	Communication systems	Disruptions
Data breaches	Insider threats or collected data	Critical information compromised
Malware	Communication networks	Data integrity compromised
DDoS attacks	Any communication traffic	Inaccessible or degrading communication with flood or traffic
GPS spoofing or jamming	GPS signals	Manipulated aircraft navigation, jammed or blocked GPS signals
Social Engineering	Phishing email	Exposure of systems to cyber threats

(F. Shaikh, 2019) presents a matrix of security threats classified by cyber threat type:

Table 3 *(F. Shaikh, 2019)* security matrix of E-enabled systems

Denial of Service (DoS) attacks	Communication Jamming attacks	Spoofing	Man-in-the-Middle & Eavesdropping attacks	In-flight cyber attacks	IT vulnerabilities
DoS on airport communication infrastructure	Attacks on GPS-based navigation aids	Lack of authentication in CPLDC	Critical information leakage	DoS jamming attacks	Lack of regulations in COTS hardware/soft ware
ATM DoS	RF transmitters interference with GPS signal reception	Message manipulation	Lack of integrity checking	Wideband jamming attacks	Traditionality of security mechanisms in modern aircrafts
Wormhole attacks	Direct interference of GPS signals	Easy impersonation	Lack of encrypted messages for ADS-B transmission	Cross-layer jamming attacks	Traditionality of IP-based networking interconnectio n in ground-based aircrafts
	Intentional interference of GPS signals	False message injection	Eavesdropping on wireless channel	Reactive jamming attacks	Lack of protection of air network traffic from unauthorized access & information leakage
	Direct jamming of GPS signals	Delay injection	Ground-based Man-in-the-Middle attacks		
	Jamming attacks on radio altimeters	Access of ICAO values via Internet	Disrupt/alter control signals		
		Generation of misleading ATC location profiles			
		Spoofing GPS readings of longitude and latitude			
		Generation & pseudo-matching real aircraft flight behaviors			

Nowadays, technologies such as Software-Defined Networks, Internet of Things (IoT), 5G communications are susceptible to various cyber threats, most of them are denial-of-service, spoofing and data leakage.

In the past three years, there have been some powerful attacks which led to global-scope consequences. The most important ones are presented in the table below.

Table 4 – Cyber-attacks in aviation

Date	Airline / Organization / Country	Type of attack	Consequences
25 May 2022	SpiceJet / India	Ransomware	**Several hours** disruption of services
April 2022	SunWing Airlines / Canada	DDoS	**4 days** extensive flight delays
March 2022	Russian CAA / Russia	APT	**65 TB** of data deleted
March 2021	SITA / Singapore Airlines / Air India Singapore, India	Data breach	**580.000** flying members data compromised (Singapore) **4.5 million** passenger data stolen
2020	VT San Antoni Aerospace, USA	Ransomware	**1 TB** data stolen, encrypted networks, 3-day system recovery
2020	easyJet, UK	Social Engineering	**2208** customers' information disclosed

5. SECURITY MECHANISMS

Depending on the cyber threat type and the attack surface, there are various security mechanisms which can be implemented.

Table 5 – Security mechanisms

Cyber threat	Attack vector	Potential damage
Unauthorized access	Disruptions	Authentication mechanisms, SRTP
Data breaches	Critical information compromised	PKI infrastructure, Radio channel integrity
Malware	Data integrity compromised	Air Traffic management security, PKI infrastructure
DDoS attacks	Inaccessible or degrading communication with flood of traffic	Radio channel integrity Traffic data control mechanisms
GPS spoofing or jamming	Manipulated aircraft navigation, jammed or blocked GPS signals	Signal monitoring and anomaly detection
Social Engineering	Exposure of systems to cyber threats	Personnel awareness

These security mechanisms must be adopted and implemented in accordance with the newer technologies and must be updated and replaced, if necessary, as emerging technologies such as artificial intelligence and quantum computers thrive.

CONCLUSIONS

It is obvious that ensuring the quality of service and security of aeronautical communications is not an easy task, but a mandatory one. Features like reliability, latency, and bandwidth or quality metrics are essential characteristics to take into consideration when designing proper aeronautical communication architecture.

If the quality of service can be ensured at a proper level by design, with security, is a more complicated issue. Security is not something that can be maintained at a very high level for a long period of time. More and more sophisticated types of attacks emerge, making it harder and harder for engineers to mitigate attacks and protect the aircraft communication infrastructure.

In conclusion, this paper emphasizes the critical importance of simultaneously addressing QoS and security in aeronautical communication networks. Achieving a balance for the two requirements is indispensable for the safe, efficient and dependable operations of aircraft systems in an increasingly security-threaten, interconnected digital environment.

REFERENCES

[1] F. Shaikh, M. Rahouti, N. Ghani, K. Xiong, E. Bou-Harb, J. Haque – "*A Review of Recent Advances and Security Challenges in Emerging E-Enabled Aircraft Systems"*, IEEE, 2019;

[2] H. Duchamp, I. Bayram, R. Korhani – "*Cyber-security, a new challenge for the aviation and automotive industries*", J. Strategic Threat Intell, 2016

[3] R. K. Rakaselaran, E. Frew – "*Cyber security challenges for networked aircraft*", IEEE, 2017

[4] M. Strohmeier, M. Shafer, R. Pinheiro, V. Lenders, I. Martinovic – "*On perception and reality in wireless air traffic communication security*", Trans. Intell. Transp. Syst, 2017

ANALYSIS OF INTERIOR NOISE IN SPECIAL PURPOSE VEHICLES

Bianca CĂȘERIU
"George Emil Palade" University of Medicine, Pharmacy, Science and Technology of Târgu Mureș, Romania (biancacaseriu@yahoo.com)
ORCID: 0000-0002-8106-1133

Petruța BLAGA
"George Emil Palade" University of Medicine, Pharmacy, Science and Technology of Târgu Mureș, Romania (petruta.blaga@umfst.ro)

DOI: 10.19062/1842-9238.2023.21.1.5

Abstract: *As vehicles have evolved from simple to complex machines with specific configurations depending on their main role, the issue of interior noise has become a topic of interest. The present paper presents a model of experimental acoustic determinations made based on standardized acoustic emission factors for a vehicle in the N2G category, taking into account the volume of the vehicle, its speed, road configuration, and the distance from the receiver. Thus, significant conclusions are reached regarding the level of acoustic emissions in the vehicle cabin. Cumulative preliminary estimates were also made for the level of interior noise in the special purpose vehicle, monitored while stationary and in motion, in order to obtain an initial picture of the cumulative impact of noise and vibrations generated by acoustic sources originating from the operation of the vehicle. Noise tests were performed under realistic operating conditions during the intensive testing period.*

Keywords: *Noise level, acoustic emission, noise test, experimental determinations, vehicle cabin, interior noise.*

1. INTRODUCTION

The upward development trend of technology and a the sudden increase in market competition within the civil and military automotive industry and the current political-military context, dictates manufacturers' obligations to fulfill the increasingly complex requirements of the user in terms of economy, comfort, ergonomics safety and environmental protection. All from above have influenced car manufacturers and the automotive industry to pay attention to technical innovations to meet the requirements related to increased cabin comfort, vehicle safety, and researchers to bring the innovation to the field [1].

The noise, vibration and harshness (NVH) of a car is among the issues of interest in the automotive industry since the decade passed [2]. Because noise crucially affects the level of passenger comfort, one of the specifications for a good quality car is one that has low interior noise level in addition to conventional features such as car performance when it comes to civilian vehicles. This becomes all the more difficult as the modern car becomes quieter; therefore, the driver's sensitivity to noise increases [3].

Regarding vehicles with special purposes, such as those used by the military, the issue of interior noise is studied from the perspective of the harmful implications on the health of the passengers. In this sense, noise becomes the source of producing a series of health problems, such as: communication and concentration difficulties; stress and irritability; sleep disorders; cardiovascular problems and negative effects on the endocrine system, on performance and work capacity that lead to a global decrease in the level of performance in activities. Also, a noise level between 35-70 dB, for a long time, to which the driver of a special purpose vehicle can be subjected leads to the appearance of fatigue, weakening of vision, difficulty in understanding speech and even causing headaches for a noise level which exceeds the value of 70 dB (such a high sound level can occur, for example, when traveling at a high speed of over 90 km/h on the highway) [4]. The harmful character of noises is amplified if they are accompanied by vibrations, just as the harmfulness of vibrations increases when they are accompanied by noises [5, 6].

The special purpose vehicles have different configurations depending on the destination, the structure of the vehicle being adjusted according to mobility criteria, specific reconnaissance activities (off-road vehicles), with or without ballistic properties, with different crew arrangements depending on the activities carried out (in the compartment, in the turret, for vehicles equipped with a turret, in the trunk). In addition to the fact that these vehicles must be equipped with additional systems to ensure the safety of passengers, they must also include ergonomic properties of the vehicle. Ergonomic properties include the ability to adjusting the interior of the vehicle to the characteristics of each individual drivers and crew members. Vehicle structure should be adapted to most users and allow individual adjustments, taking this into account dimensions, in order to: better visibility from vehicle, higher comfort, comfortable seat, lighter better driving, access and use of controls and devices, better sound and heat insulation, reduced vibration effect and driver fatigue.

Off-road vehicles include special engine vehicles that are part of the N2G category, classified in accordance with RNTR 2, special purpose vehicles that are used both on regular roads, in normal weather conditions and on difficult terrain and in complex weather conditions, for specific activities, usually used by the military. For these reasons, especially due to their use in complex weather missions and activities and difficult conditions, it is necessary that manufacturers and researchers who develop and bring improvement concepts on these kinds of vehicles, pay special attention to testing and adjustment models to comply with the standards existing during design and development of test models, in view ensure that the user's health is protected [7,8].

A problem specific related to special purpose off-road vehicles regarding the consideration of the previously listed requirements comes from the fact that they have a long life span, which can causes them to lag behind automotive industry standards which are constantly changing [9].

Thus, the present paper presents a strategy for monitoring and measuring as well as obtaining important data regarding the acoustics of the passenger compartment of special purpose vehicles, with the aim of outlining new research directions for the selection of the best available techniques, with the aim of making contributions for the additional mitigation of the impact potential noise on the passengers, as well as the implementation of a strategy that leads to the improvement of the interior acoustic comfort level.

2. THE PERCEPTION OF NOISE BY THE HUMAN AUDITORY SYSTEM

The main human auditory organ, specialized in the transformation of sound signals and noise, in general, into auditory sensations, is the ear.

The human ear, divided into the external ear, the middle ear and the inner ear, has the role of transforming the pressure variations that accompany a sound wave into electrical signals, which are finally transformed in the cortex into auditory sensations.

The human auditory system has the ability to do, in this process of transforming an air pressure variation into sensation, several analysis processes, an analysis in frequency, distinguishing different frequency sounds, an analysis in intensity, which refers to the fact that it distinguishes the different amplitude of two sounds of the same frequency, and can also amplify or attenuate perceived sounds that lie in different frequency bands. We can also talk about the situation where a sound with a certain level of sound intensity can mask another sound with a lower intensity. The mechanisms underlying the creation of an auditory sensation are extremely complex, hearing essentially having a valid general character, but also a certain particular character [10,11].

About the human ear it can be said that it perceives sounds that are located in a wide frequency band, more precisely from 16 Hz - 16000 Hz. Below and beyond these limits, the human being has no auditory sensation. With age, the sensitivity of the human auditory organ decreases. Any physiological or traumatic condition of it can lead to hearing impairment or even deafness. Also, prolonged exposure to noises with high acoustic levels inevitably lead to hearing loss, which can have different degrees [12].

The frequency analysis of sounds takes place in the inner ear, where the muscle bundles of the basilar membrane behave like the strings of a piano, being excited by different frequencies [13].

The threshold of audibility is the minimum at which the human ear perceives a sound, the level at which a person has auditory sensation. This threshold depends on the frequency of the emitted sounds, for example at the frequency of 1 kHz, the threshold value is 2 dB, between 2000-6000 Hz due to the amplifications in the ear, the perception drops below this level, appearing a level that shows that the auditory sensation is excited by variations of the pressure below the reference value p=20μPa [14].

The audibility range is limited in terms of the level of two curves, the audibility threshold curve p_A and the pain threshold curve p_D, and in terms of the band frequency range 16 Hz-16 kHz. For a normal ontological listener, the pain threshold shows an approximately constant plateau, with a higher sensitivity of the ear in the amplification zone 2000-6000 Hz. The pain threshold located in the area of a level of 120 dB, shows that the sensitivity area, under normal conditions, of the auditory apparatus extends over an extremely large beach, from 20 μPa to 20 Pa. Although in relation to the atmospheric pressure p_{atm} =100 kPa, the pressure value corresponding to the pain threshold pressure seems small, it is a pressure variation, a dynamic quantity. The forces that act on the sensitive mechanisms of the middle ear are very small, if we refer to the area of the eardrum which is about 1 cm^2, it supports in the area of the pain threshold 0.02 N and a force a million times smaller, the case of the threshold of audibility [15].

The different perception of sounds by the human ear compared to measuring devices required the creation of different scales for measuring the acoustic pressure level depending on the field in which they are used, present in the specialized literature. The adaptation of the measurement system, by which real values are obtained by objectively measuring the sound pressure level, according to the auditory sensation of the listener, led to the introduction of corrections by means of standardized weighting scales with the designations A, B, C and D, which to take into account the criteria established after the experiments. A weighting scale is a set of numerical values by which the objective sound pressure level measured at different frequencies is corrected.

Since, at low frequencies < 200 Hz the sounds are poorly perceived, the corrections are negative, and in the range 2000-6000 Hz, where the sensitivity of the ear is maximum, the corrections are positive [16]:

- The A scale is the one that comes closest to human auditory perception and includes significantly higher corrections for the low frequency spectrum, for normal sound intensity levels, <60 dB.
- The B scale, follows the subjective perception of the human ear, for moderate levels of the acoustic intensity level, > 60 dB, for which the sensitivity of the human ear flattens.
- The C scale is the scale that comes closest to the measured sound intensity level, introducing corrections only if the noises are very loud.
- The D scale is studied for the study of aircraft noise and introduces significant corrections in the frequency band where the ear's sensitivity is maximum 2000-6000 dB

The corrections that are introduced in the weighted scales lead to an overall decrease in the sound level, compared to the actual, measured sound level. That is why when acoustic level values are presented, the scale in which they were weighted must also be specified [17].

3. DETERMINING THE NOISE LEVEL INSIDE SPECIAL PURPOSE VEHICLES

3.1 Technical generalities regarding the tested vehicle

In this study, data obtained based on experimental determinations on off-road special purpose vehicles are presented, one of which is the Panhard vehicle. Tests were carried out on vehicles of configurations in this category, creating a database, which will later be interpreted, presenting significant conclusions from a scientific point of view.

One of the tested models, for which the obtained values are of interest from the point of view of the noise issue, is presented in Fig.1 a) and b), while Table 1 presents general technical information about this off-road vehicle.

Table 1

General information	Model Panhard
Type	Off road
Category	N2G special vehicle
Mass of the vehicle	5050 kg
Drive	4x4
Pneumatics	255/100R16 126K
Speed	3500 rpm
Nominal engine power	122 KW
Seats	4

(a)

(b)

FIG. 1 The vehicle subject to experimental determinations

3.2 Experimental testing methodology

The noise produced in the passenger compartment of the special vehicle types analyzed is measured with the vehicle in motion and with the vehicle stationary, in accordance with ISO 5128: 1980 on the measurement of noise inside motor vehicles. In the case of a hybrid electric vehicle whose internal combustion engine cannot operate when the vehicle is stationary, the emitted noise level shall only be measured in motion.

The equipment used to measure the sound level is a precision sound level meter or an equivalent measuring system meeting the requirements for instrument class 1 (including the wind shield recommended by the manufacturer, if applicable). These requirements are described in the International Electrotechnical Commission (IEC) standard "IEC 61672-1:2002: Precision sound level meters", second edition. Measurements are made using the "quick" response of the acoustic measuring instrument and the "A" weighting curve also described in "IEC 61672-1:2002". If a system is used that includes periodic A-weighted sound pressure level monitoring, readings shall be taken at time intervals of no more than 30 ms (milliseconds). For the cases studied, intervals of 60 s were taken into account.

Before carrying out the experimental determinations for the passenger compartment of special purpose vehicles, an analysis of the research in the field was necessary: articles, books and various other publications and not least of some international standards that refer to the acoustics of the vehicle passenger compartment. Based on the exploratory approach regarding the bibliography of the study, a gap was identified regarding the documentation made by researchers and specialists in acoustics and vibrations in our country [18-20]. Thus, the research methodology is carried out according to the block diagrams in the Fig.2, taking into account compliance with the standards of acoustic determinations in force.

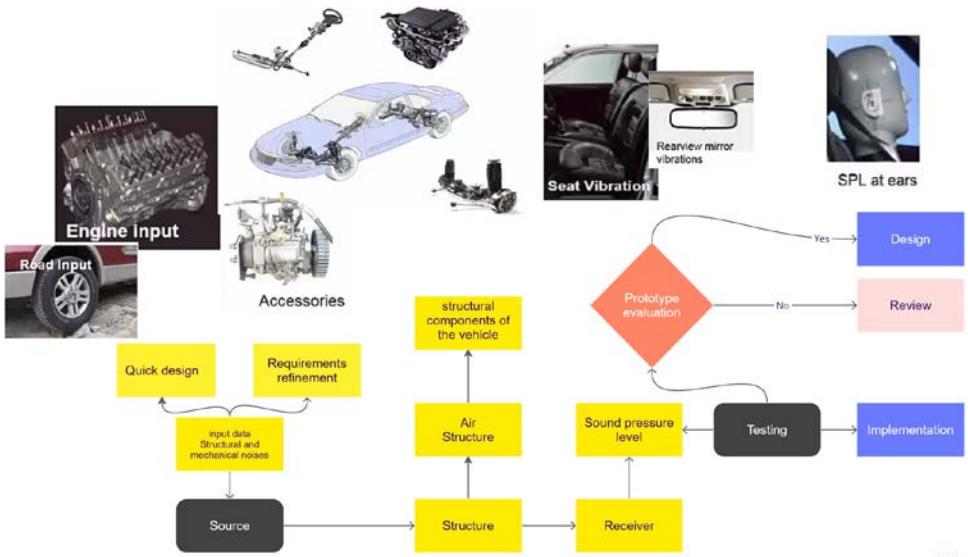

FIG. 2 Block diagram of the noise analysis in the vehicle cabin.

In the block figure related to the research methodology, the input data and the output data of the complex dynamic system are represented, regarding the problem of interior noise in vehicles. The noise from prominent noise sources as a result of the operation of the vehicle propagates in its structure. Also as a result of exploitation, another prominent source of noise comes from the interaction of the vehicle with the external environment (air) as well as structural noise. At the receiver, a sound is perceived as acoustic pressure. Based on the experimental determinations, the equivalent acoustic pressure values were determined. As a result of the results obtained, a prototype is evaluated or improved to fit the acoustic norms recommended by the standards.

The realization of some improvements regarding the acoustics of the interior of the vehicles is based on an integrated system: spectral analysis of the noise produced inside the vehicles, creation and management of the research input database, virtual modeling based on advanced mathematical algorithms, numerical testing of the effectiveness of noise mitigation, feedback system of design, model making, testing and verification, testing and verification in real conditions, achieving the improvement of the NVH properties of the vehicle interior.

The integrated system for the analysis of the interior acoustics of the vehicle is based on factors of a subjective nature (receiver) and of an objective nature (frequency analysis using specific acoustic descriptors or finite element analysis).

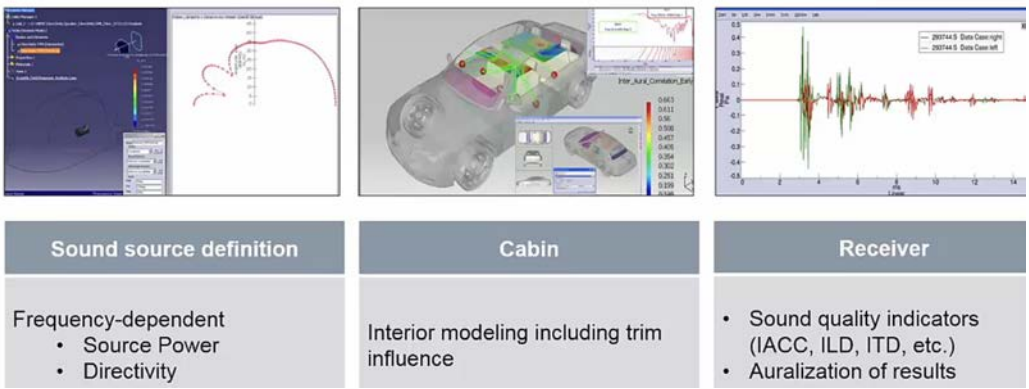

FIG. 3 Integrated system proposed for the interpretation of results

The testing methodology proposed for the experimental determination of the noise level in the cabin of special purpose vehicles is preceded by developed theoretical models: the finite element method and mathematical formulas. This is how the acoustic pressure level is determined inside special purpose vehicles, in the N2G category. This involves: preparation of the working environment, namely the track for making measurements, which is a straight asphalted ground for a length of 500 m, without being covered by snow, tall grass; in the immediate vicinity of the test track there are no obstacles at a distance of 20m (buildings, vehicles, large objects), which could influence the reflection of sound waves; a measuring device was further identified, meeting the requirements for class 1 instruments, weighted in frequency and time in the A scale, namely a sound level meter; the next step is to identify the environmental conditions with the anemometer, a temperature of 25 ^{0}C was identified in the reference range of +5 and +40 ^{0}C and a wind speed of 3m/s below the reference wave level of 5m/ s; also before and after each measurement the sound measuring device was calibrated and the background noise was measured in an interval of 10 seconds; finally, the measuring devices were positioned and the values of the interior acoustic pressure level were determined, for different engine operating speeds of special purpose vehicles.

The obtained data were processed and constituted in a database, which is analyzed later.

3.3 Determining the noise level inside special purpose vehicles

For each speed, 100 values of the equivalent continuous sound level were obtained, in an interval of 60 s. The measurements were performed on a test track characterized by terrain, without obstacles, these being located at a distance of at least 20 m from the test track.

a) Measurement method. The stages for the N2G category vehicle, Panhard type, are presented. The noise produced by the type of vehicle under measurement is measured with the vehicle stationary, for various engine operating speeds.

b) Equipment required for measurements. The following devices were used, necessary to perform the measurements: PC system (laptop); Sound analysis software; Sound level meter (SLM), accuracy class 1, with frequency and time weighting, according to the specifications of international standards such as IEC 61672 – 1, instrument (portable) which is designed to measure sound pressure levels in a standardized way. It responds to sound in roughly the same way as the human ear and provides objective, reproducible measurements of sound pressure levels. This sound level meter comprises a microphone, a preamplifier, signal processing and a display. The microphone converts the acoustic signal into an equivalent electrical signal. The most suitable type of microphone for sound level meters is the condenser microphone, which combines precision with stability and reliability. The electrical signal initially produced by the microphone being very low is then amplified by a preamplifier before entering the main processor. Signal processing includes frequency and time weighting as specified by international standards such as IEC 61672 – 1; Multimeter for measuring wind speed and air temperature with an accuracy of ±(0.1m/s+5% of the measured value - 0 to 2 m/s), ±(0.3m/s+5% of the measured value - 2 to 15 m/s).

c) Verification of compliance with the requirements. The conformity of the instruments for acoustic measurements is verified by the existence of a valid certificate of conformity. A certificate of conformity is considered valid if the certification of conformity with the standards has been carried out within the last 12 months for the sound calibration device and within the last 24 months for the

measuring system. All compliance tests must be performed by a laboratory authorized to carry out calibrations corresponding to the specific standards in force.

d) Calibration of the entire acoustic measurement system for the series of measurements. At the beginning and at the end of each series of measurements, the entire acoustic measurement system shall be checked by means of an acoustic calibration device that complies with the requirements for acoustic calibration devices of accuracy class 1 according to standard IEC 60942:2003. Without any other adjustment, the difference between readings must be less than or equal to 0.5 dB. If this value is exceeded, the measurement results obtained at the last satisfactory previous check are not considered valid.

e) Measurement conditions. The surface of the test track and the dimensions of the test polygon comply with the ISO 10844:2011 standard. The range surface is not covered with loose snow, tall grass, lumps of dirt or ash. There must be no obstacle that can affect the sound field in the vicinity of the microphone and the sound source. The observer making the measurements must position himself so as not to affect the readings of the measuring instrument. Measurements are not made in adverse weather conditions. It must be ensured that the results are not affected by wind gusts. Meteorological measuring instruments must be positioned in close proximity to the test area at a height of 1.2 m ± 0.02 m. The measurements are carried out when the ambient air temperature is between + 5 °C and + 40 °C. No tests shall be performed if, when measuring noise, the wind speed, including gusts, at the height of the microphone exceeds 5 m/s. During the noise measurement period, representative values for temperature, wind speed and direction, relative humidity and barometric pressure are recorded. Any peak noise value that appears to be unrelated to the overall sound level characteristics of the vehicle is ignored in the reading. The background noise shall be measured over a 10-second interval immediately before and immediately after a series of vehicle tests. The measurements are carried out with the same microphones placed in the same positions as during the test. The maximum A-weighted sound pressure level is recorded. The position of the sound level meter has a coordinate in the horizontal plane of 0.7±0.04 m, and in the vertical plane 0.2±0.02 m, as in the Fig. 4. These reference coordinates are measured according to the plane of symmetry, in the vertical plane of the driver's seat. The position of the microphone must be in a horizontal plane, mounted so that it is not influenced by the vibrations of the vehicle. Before starting the measurements, bring the engine to normal operating conditions.

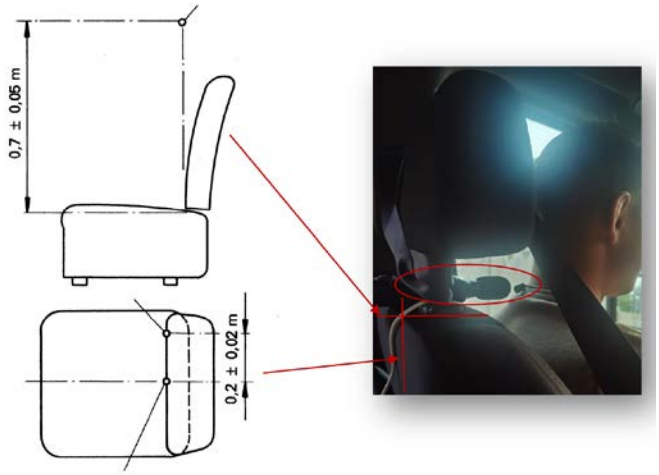

FIG. 4 Position of microphones for indoor noise determination according to ISO 5128:1980.

f) Noise measurement in the passenger compartment of the special purpose vehicle. The noise level measurement is carried out at a standstill with the engine running. Measurements are taken without any trailer.

g) Vehicle category: N2G, special purpose vehicle.

h) Work method and results obtained. As a result of the experimental determinations, the following values of the internal noise level were obtained while stationary for different operating speeds of the engine:

- **Speed of n=800 rpm:**

Table 1. Synthesis of sound level values, obtained over 60s, at n=800 rpm of the engine (at idle), stationary

n[rot/min]	800	800	800	800	800	800	800	800	800
Leq [dBA]	56.4	58.0	57.1	57.9	56.9	57.4	57.6	56.6	57.1
n[rot/min]	800	800	800	800	800	800	800	800	800
Leq [dBA]	56.8	57.1	56.7	57.1	57.4	56.7	57.5	57.5	57.1

The average value for the noise level at n=800 rpm is: 57.78 dB(A).

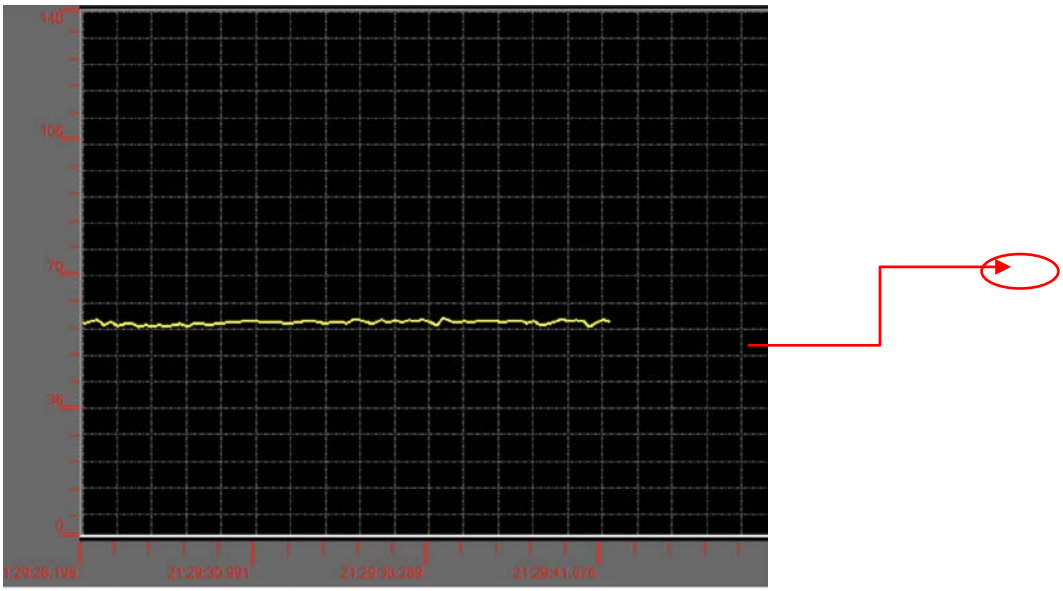

FIG. 5 Time dependence graphs of interior noise levels, for one combat all-terrain vehicle, at n=800 rpm, stationary

- **Speed of n=1500 rpm:**

Table 1. Synthesis of sound level values, obtained over 60s, at n=1500 rpm of the engine (at idle), stationary

n[rot/min]	1500	1500	1500	1500	1500	1500	1500	1500	1500
Leq [dBA]	67.4	69.3	67.7	68.7	69.1	67.3	68.3	67.5	69.7
n[rot/min]	1500	1500	1500	1500	1500	1500	1500	1500	1500
Leq [dBA]	69.9	68.5	68.8	68.8	69.4	68.3	67.5	69.7	69.9

The average value for the noise level at n=1500 rpm is: 69.3 dB(A).

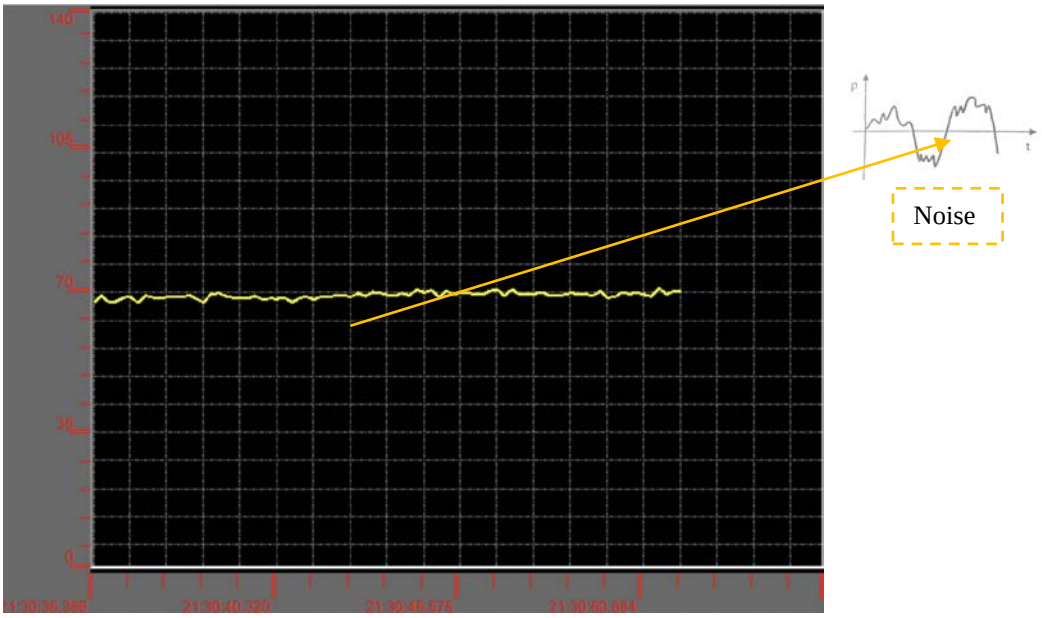

FIG. 5 Time dependence graphs of interior noise levels, for one combat all-terrain vehicle, at n=1500 rpm, stationary

- **Speed of n=2000 rpm:**

Table 1. Synthesis of sound level values, obtained over 60s, at n=1500 rpm of the engine (at idle), stationary

n[rot/min]	2000	2000	2000	2000	2000	2000	2000	2000	2000
Leq [dBA]	71.8	78.4	78.2	72.1	72.5	71.0	71.5	70.5	71.4
n[rot/min]	2000	2000	2000	2000	2000	2000	2000	2000	2000
Leq [dBA]	71.3	71.9	71.8	71.9	71.9	72.0	74.0	75.0	74.6

The average value for the noise level at n=2000 rpm is: 74.44 dB(A).

FIG. 6 Time dependence graphs of interior noise levels, for one combat all-terrain vehicle, at n=2000 rpm, stationary

NOTE: For each speed, 100 values of the equivalent continuous sound level were obtained, in an interval of 60 s. The measurements were performed on a test track characterized by terrain, without obstacles, these being located at a distance of at least 20 m from the test track.

4. INTERPRETATION OF EXPERIMENTAL RESULTS

Analyzing the results obtained from the experimental determinations, the dependence graph of the internal acoustic pressure level can be drawn according to the speed.

A comparative analysis is also carried out between a regular off-road configuration vehicle subject to the same test methodology and the special purpose vehicle, based on the values obtained.

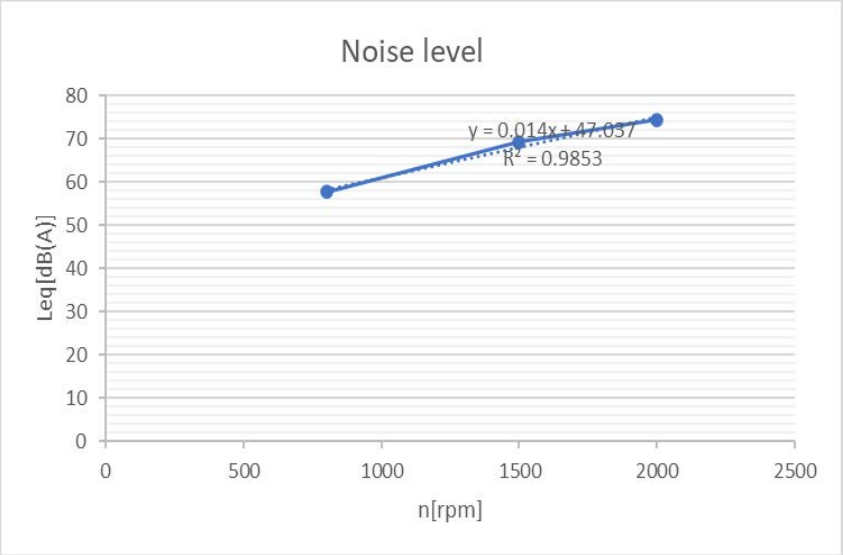

FIG. 7 Dependence graphs of interior noise levels, for the tested combat all-terrain vehicle.

The acoustic pressure values increase from the average value of 57.78 dB(A), at the speed of n=800 rpm, to 69.3 dB(A) at the speed of n=1500 rpm, up to 74.44 at n=2000 rpm min. It is also found that there are pressure peaks that reach up to 78.4 dB(A). The dependent equation for the definition of the average values of the three average values for the revolutions: 600 rpm, 1500 rpm and 2000 rpm is: y=0.014x+47.037.

Analyzing the graph drawn in **fig. 7**, it can be stated that the values of the internal acoustic pressure level obtained while stationary, increase significantly with the motor speed.

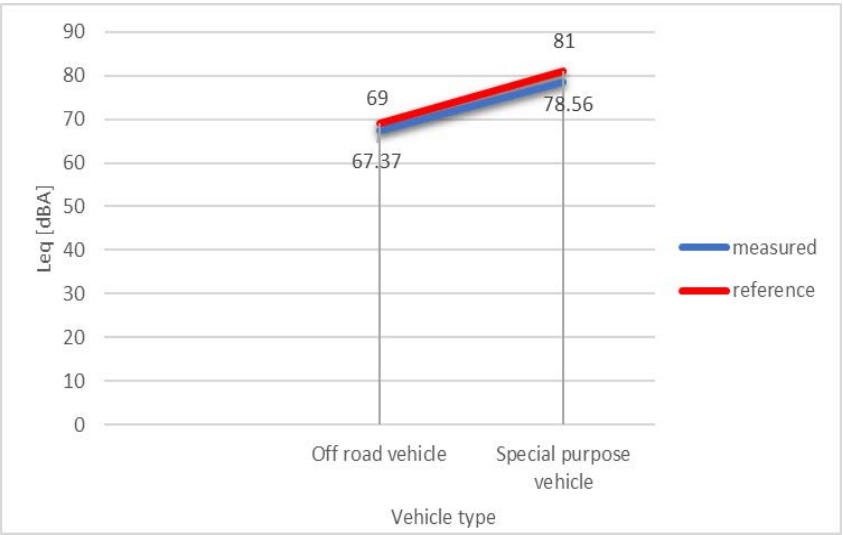

FIG. 8 Dependence graphs of interior noise level, for the combat all-terrain vehicle and off road vehicles. Comparison.

According to the graph drawn in Fig.8, based on the measurements performed on an off-road vehicle and a special purpose vehicle, it can be seen that the values of the acoustic pressure level in the passenger compartment are located below the reference line of the values allowed by the standard, but they are close in values, the difference being only 2 dB-3dB. The graph represents the average values of Leq at 2500 rpm. Special purpose vehicles show values of more than 10 bB, stationary compared to regular off-road vehicles. This fact implies equipping them with anti-noise headphones, as well as taking additional measures to reduce the noise so that it is not harmful to the passengers.

CONCLUSIONS

Synthesizing the predictive theoretical studies through calculation methods as well as the analyzed experimental results, the following conclusions are presented:

- For the off-road vehicle of the N2G special vehicle category, the sound pressure level in the passenger compartment, when stationary, can reach up to 74.44 dB.
- Based on the experimental determinations, it was found that there are pressure peaks that reach values of up to 78.2 dBA, or even values of 78.4 dBA. High indoor sound pressure values even for a short time affect passengers in a negative way.
- According to the experimental determinations of noise inside special purpose vehicles, an average interior acoustic pressure value of 57.78 dB(A) at 800 rpm was obtained when stationary, 69.3 dB(A) at 1500 rpm rpm and 74.44 dB(A) at 2000 rpm.
- Special purpose vehicles have higher interior acoustic pressure values than classic off-road vehicles, which is also due to their special purpose.
- The acoustic background associated with the passenger compartment of the vehicle both in motion and stationary, in the test conditions, continuously contributes to the noise profile perceived by the passengers.
- At the same time, the interior acoustic pressure values are not an indicator of acoustic comfort, but they are constitutive in determining it.
- In the operation of motor vehicles on public roads, transient sources (such as traffic) will contribute significantly to the noise profile in the cabin perceived by passengers, leading to values that exceed the permissible limits.
- The noise variations determined as a result of the experimental measurements in the passenger compartment of the vehicle lead to discomfort and have harmful effects on the passengers. A noise level between 35-70 dB, for a long time, to which the driver of a vehicle can be subjected leads to the appearance of fatigue, impaired vision, difficulty in understanding speech and even causes headaches for a noise level exceeding the value of 70 dB.
- A monitoring and measurement strategy is presented as well as important data regarding the acoustics of the passenger compartment of special purpose vehicles, together with the selection of the best available techniques, with the aim of contributing to the further mitigation of the potential sound impact on passengers, as well as the implementation of a strategies to improve the indoor acoustic comfort level.

REFERENCES

[1] B. Cășeriu, P. Blaga, Automotive Comfort: State of the Art and Challenges. In: Moldovan, L., Gligor, A. (eds) The 16th International Conference Interdisciplinarity in Engineering. Inter-Eng 2022. Lecture Notes in Networks and Systems, vol 605. Springer, Cham. https://doi.org/10.1007/978-3-031-22375-4_30, 2023;

[2] P. Gardonio, Boundary Layer Noise – Part 2: Interior Noise Radiation and Control. In: Camussi, R. (eds) Noise Sources in Turbulent Shear Flows: Fundamentals and Applications. CISM International Centre for Mechanical Sciences, vol 545. Springer, Vienna. https://doi.org/10.1007/978-3-7091-1458-2_7, 2013;

[3] L. Yi, H. Huang, G. Chang, D. Luo, C. Xu, Y. Wu, and J. Tang. 2022, *Research on Low-Frequency Noise Control of Automobiles Based on Acoustic Metamaterial*, Materials 15, no. 9: 3261. https://doi.org/10.3390/ma15093261, 2022;

[4] V. Baskov, A. Ignatov, E. Isaeva, *A Mechanism for assessment of automobile noise impact on drivers and passengers*, Transportation Research Procedia, Volume 36, Pages 33-36, ISSN 2352-1465, https://doi.org/10.1016/j.trpro.2018.12.039, 2018;

[5] A.V. Pobedin, V.V. Shekhovtsov, A.A. Dolotov, *Computational Probabilistic Evaluation of Passenger, Cars Noise Level*, Procedia Engineering, Volume 206, Pages 1558-1563, ISSN 1877-7058, https://doi.org/10.1016/j.proeng.2017.10.677, 2017;

[6] V. A. Strekalov, & R. Shaimuhametov, N*oise mapping inside a car*, IOP Conference Series: Materials Science and Engineering (Vol. 240, No. 1, p. 012066). IOP Publishing, doi http://10.1088/1757-899X/240/1/012066, 2017;

[7] Z.S. Liu, C. Lu, Y.Y. Wang, H.P. Lee, Y.K. Koh, K.S. Lee, Prediction of noise inside tracked vehicles, Applied Acoustics, Volume 67, Issue 1, Pages 74-91, ISSN 0003-682X, https://doi.org /10.1016/j.apacoust.2005.05.003, 2006;

[8] J.P. Coyette, *The use of finite-element and boundary-element models for predicting the vibro-acoustic behaviour of layered structures*, Advances in Engineering Software, Volume 30, Issue 2, Pages 133-139, ISSN 0965-9978, https://doi.org/10.1016/S0965-9978(96)00041-5, 1999;

[9] C.S. JOG, Topology design of structures subjected to periodic loading, Journal of Sound and Vibration, Volume 253, Issue 3, Pages 687-709, ISSN 0022-460X, https://doi.org/10.1006/jsvi.2001.4075, 2002;.

[10] I. Akhoun, S. Gallégo, A. Moulin, M. Ménard, E. Veuillet, C. Berger-Vachon, L. Collet, H. Thai-Van, The temporal relationship between speech auditory brainstem responses and the acoustic pattern of the phoneme /ba/ in normal-hearing adults, Clinical Neurophysiology, Volume 119, Issue 4, Pages 922-933, ISSN 1388-2457, https://doi.org/10.1016/j.clinph.2007.12.010, 2008;

[11] J. Cunningham, T. Nicol, C. King, S.G Zecker, N. Kraus, *Effects of noise and cue enhancement on neural responses to speech in auditory midbrain, thalamus and cortex*, Hearing Research, Volume 169, Issues 1–2, Pages 97-111, ISSN 0378-5955, https://doi.org/10.1016/S0378-5955(02)00344-1, 2002;

[12] E.M Glaser, C.M Suter, R Dasheiff, A Goldberg, *The human frequency-following response: Its behavior during continuous tone and tone burst stimulation*, Electroencephalography and Clinical Neurophysiology, Volume 40, Issue 1, Pages 25-32, ISSN 0013-4694, https://doi.org/10.1016/0013-4694(76)90176-0, 1976;

[13] J. Dora, D. Wojcieszak, D. Kaczmarek, M. Mazur, A. Aksenczuk, New theory of acoustic signal detection in the inner ear – An explanation of bifilar structure of the cochlea, Medical Hypotheses, Volume 140, 109636, ISSN 0306-9877, https://doi.org/10.1016/j.mehy.2020.109636, 2020;

[14] S.K. Scott, I. S. Johnsrude, The neuroanatomical and functional organization of speech perception, Trends in Neurosciences, Volume 26, Issue 2, Pages 100-107, ISSN 0166-2236, https://doi.org/10.1016/S0166-2236(02)00037-1, 2003;

[15] Jos J Eggermont, Between sound and perception: reviewing the search for a neural code, Hearing Research, Volume 157, Issues 1–2, Pages 1-42, ISSN 0378-5955, https://doi.org/10.1016/S0378-5955(01)00259-3, 2001;

[16] W. A. Yost, Auditory image perception and analysis: The basis for hearing, Hearing Research, Volume 56, Issues 1–2, Pages 8-18, ISSN 0378-5955, https://doi.org/10.1016/0378-5955(91)90148-3, 1991;

[17] F. Prévost, M. Laroche, A.M. Marcoux, H.R. Dajani, Objective measurement of physiological signal to-noise gain in the brainstem response to a synthetic vowel, Clinical Neurophysiology, Volume 124, Issue 1, Pages 52-60, ISSN 1388-2457, https://doi.org/10.1016/j.clinph.2012.05.009, 2013;

[18] A.V. Bulibașa, M. D. Stanciu, and J. Timar. *Măsurarea nivelului de zgomot produs de motociclete area nivelului de zgomot produs de motociclete*, Buletinul AGIR 28.1, ian-mar2023, Vol. 28 Issue 1, p20-28. 9p. 2023;

[19] C. Doru, Studii și cercetări privind îmbunătățirea unor parametri de confort în sisteme de transport. Diss. Universitatea Politehnica Timișoara, 2018;
[20] C.N. Badea et al., Z*gomotul produs de vehiculele feroviare în curbe*, Sinteze de Mecanica Teoretica si Aplicata 10.1 pp.11-24, 2019.

ERGONOMIC RISK ASSESSMENT IN CERTAIN INDUSTRIAL FIELDS USING THE QEC AND RULA METHODS

Adrian ISPĂȘOIU
"Transilvania" University of Brașov, Romania (adrian.ispasoiu@unitbv.ro)
ORCID: 0000-0002-2613-8337

Ioan MILOSAN
"Transilvania" University of Brașov, Romania (milosan@unitbv.ro)

DOI: 10.19062/1842-9238.2023.21.1.6

Abstract: *In many industrial activities carried out by workers, some parts of the human body or even the body as a whole are overused to a degree that can affect the health of the workers. Established ergonomic risk assessment methods include QEC and RULA, and these methods aim to assess the risk factors that may cause workers to develop WMSDs. The purpose of this study is to evaluate the ergonomic risks related to workers' bodily postures when they work on conveyor belts. By using the QRC and RULA methods comparatively, it is possible to see which of the two tools are more suitable for evaluation in this type of activity and which of the two methods offers a more accurate diagnosis. The ERGOWORK version 2.7B software application was used for data entry and processing, which implements both methods. Based on the results obtained, conclusions and recommendations were drawn regarding the workers' workstations, and these can be materialized in the redesign of the work equipment and/or the replacement of the worker, in the execution of certain operations, by automatic machines.*

Keywords: *ergonomics, QEC, RULA, OHSS, WSDs, risk assessment*

1. INTRODUCTION

It is already known that one of the most frequent causes of occupational diseases are musculoskeletal disorders. Work-related musculoskeletal disorder (WMSD) is a term that refers to any disorder that affects muscles, nerves, the supporting bone structure of the body, tendons as a result of performing an activity [1].

In the last 10 years, there has been an increase in the number of cases of musculoskeletal disorders among workers in the industrial field. Although technology has evolved and has a high degree of human adaptability, workers are still exposed to a number of ergonomic risk factors.

The evolution of technology has eliminated or improved some work situations in which workers were affected, but on the other hand, it has increased the pace of work and physical and mental demands on workers in certain areas of the production chain, as workers it must keep up with technology and not slow down production. At the same time, the safety and health specialists tried to identify these ergonomic risk factors as accurately as possible and to evaluate them, in order to find the best improvement and control measures for these risk factors.

In this regard, various methods of ergonomic risk assessment are used internationally. Some of these methods, although using their own parameters that are different from other methods, seem to be similar. And then the question arises which method of ergonomic risk assessment is more appropriate.

In this study, we compared, using the same case study, two methods of ergonomic risk assessment that are quite widely used internationally. These two methods are QEC [2-5] and RULA [6, 7]. Both methods, The QEC (1998) and RULA (1993) methods mainly aims at the evaluation of risk factors during the activities, which have been found to have a major impact on the occurrence WMSD, such as biomechanical factors (improper body postures, repetitive movements, force exertion for lifting and carrying heavy loads, static work, bending and continuous rotations and task duration) and environmental factors (which are including temperature, psychological and organizational factors including high production demand, low control and lack of social support as well as personal factors like gender and age).

2. METHODS IN ERGONOMIC RISK ASSESSMENT IN INDUSTRY

The comparison of the two observation techniques was also based on a study of the literature. The authors of this study conducted several relevant studies and studied much of the literature (including electronic database search) that was considered in this study.

2.1. Ergonomic Risk Assessment

Ergonomics is a science that studies the interactions of people with the work environment, taking into account the functional characteristics, abilities and limitations of people in the design of work systems, so that people can work with safety, comfort and efficiency parameters, [8]. The assessment of ergonomic risks is particularly important at the workplace because by identifying the risks that can affect workers, preventive and control measures for these risks can be taken in advance [9].

2.2. Work Posture

The posture of the body during the activity is especially important. The further away from the neutral position the position, the higher the risk of illness. To this are added the multiplication factors such as: the force exerted, the repeated movements, the duration of the effort, etc. A good working posture is determined by the movement and positioning of the body parts during work, corroborated with the duration in which the worker stays in this posture.

2.3. Workstation Design

The design and arrangement of the workstation must take into account the avoidance of awkward positions for workers. The design of the workstation must be able to adjust to the workers to provide comfort, safety and the best work performance. The dimensions of the workstation must be able to be adjusted and adapted to the anatomy and movement needs of the worker's body.

2.4. QEC

Quick Exposure Check (QEC) is a method of occupational risk assessment associated with muscular disorders that analyzes and evaluates how the trunk, shoulders, arms, wrists and neck are affected during activities. [2-5]. According to the QEC methodology, these main parts of the body that are evaluated in terms of ergonomic risks are presented in Table 1.

QEC contributes to the identification of problems related to ergonomics and, through this, the necessary measures can be taken to prevent the occurrence of WMSDs (Work-related Musculoskeletal Disorders), acting on causes such as: repetitive movements, compressive forces, incorrect posture and duration of effort [8].

Table 1. Body parts that may be affected by ergonomic risk factors

Notation in the QEC questionnaire	Body parts	In relation with
A, B	Back	Back posture, weight, duration, frequency
C, D	Shoulder/Arm	Height, weight, duration, frequency
E, F	Wrist/hand	Repeated motion, force, duration, wrist posture
G	Neck	Neck posture, duration, visual demand

The QEC method combines the assessment of the posture observed by the researcher and the factors related to the exerted force, visual precision, stress, from the perspective of the operator or the respondent.

The total load rating can be calculated by combining the estimate made by the assessor (A-G) and the workers (H-P).

The exposure level (E) is calculated based on the percentage resulting from the total exposure of the score thus calculated (X) with a total maximum score (X max) [10], as presented in equation (1).

$$E(\%) = \frac{X}{X_{max}} x100\% \quad (1)$$

Explanation of terms:

X = Total score, obtained from sum of scores (back + shoulder/arm + wrist/hand + neck);

Xmax = Maximum total score for working posture (back + shoulder/arm + wrist/hand + neck);

Xmax is a constant for certain type of tasks. If the body is in a static position (sit or stand without repetition and relatively lower load) then the maximum score is: Xmax = 162.

The maximum score: Xmax = 176, gave when the worker did manual handling such us lifting, pushing, pulling and carrying loads.

2.5. RULA

RULA was developed by Dr. Lynn Mc Atamney and Dr Nigel Corlett [6]. RULA is an ergonomic risk assessment method that investigates and assesses the working position of the upper body.

This method is used to assess work posture by analyzing a posture sequence from a work cycle, the posture sequence that is considered to have the greatest risk to workers, and then the score is calculated.

QEC and RULA are composed of manual procedures to obtain results and scores based on observations and specific tabular parameters.

Applying these procedures takes about 5 minutes for the observer to calculate scores for a single task. When the tasks to be evaluated are not many, this time is acceptable. But, in general, in real production environments, the number of tasks to be analyzed is large, and then the application of QEC and RULA methods can be time-consuming. [11, 12].

Table 1 shows the main characteristics of the two methods QEC and RULA. With X it was noted that the respective method takes into account the respective characteristic, even to a greater or lesser extent, and with the sign – it was noted that the respective characteristic is not represented in the method.

Table 2. General characteristics of QEC and RULA

Assessment factors	QEC	RULA
Posture		
Back	X	X
Shoulder/Arm	X	X
Wrist/Hand	X	X
Neck	X	X
Legs	-	X
Static posture	X	X
Maximum weight handled	X	X
Time	X	X
Repeated movements / frequency	X	X
Maximum force level exerted by one hand	X	-
Visual demand	X	-
Drive a vehicle at work	X	-
Vibrations	X	-
Work pace	X	-
Stress	X	-

3. DATA COLLECTION FOR QEC & RULA

To collect data in this study, where used several techniques, such as: observing the posture of the workers when they perform the activities, interviewing the workers regarding the ease or difficulty with which they perform these activities and evaluating the posture of the workers during the performance of the tasks, taking into account the posture that can affect the worker the most. Before that, there were discussions with the supervisor and the employees to understand the production process, the work processes and the activities carried out by the workers, especially the activities that affect them the most.

Fig. 1 shows the conveyor belt, the trolley, the dimensions of the work space and the posture of the worker can be observed during the transfer of the parts from the conveyor belt to the trolley.

FIG. 1. Conveyor belt, trolley, workspace dimensions

Figure 2 shows the position of the worker when he takes over the parts from the conveyor belt and Fig. 3 shows the worker's position when placing the parts on the trolley.

FIG. 2. The position of the worker when he takes over the parts from the conveyor belt

FIG. 3. The worker's position when placing the parts on the trolley

By observing the work stations, as can be seen in Fig. 2 and 3, it becomes obvious that in order to move the parts from the conveyor belt to the trolley, the workers practically rotate their torso by about 180 gr, tilt their torso, stretch after the pieces, and if they have to place the parts at the bottom of the conveyor, then they tend to tilt their neck too much.

In Fig. 4 (a) and (b) values for the Observer's assessment and Worker's assessment are presented.

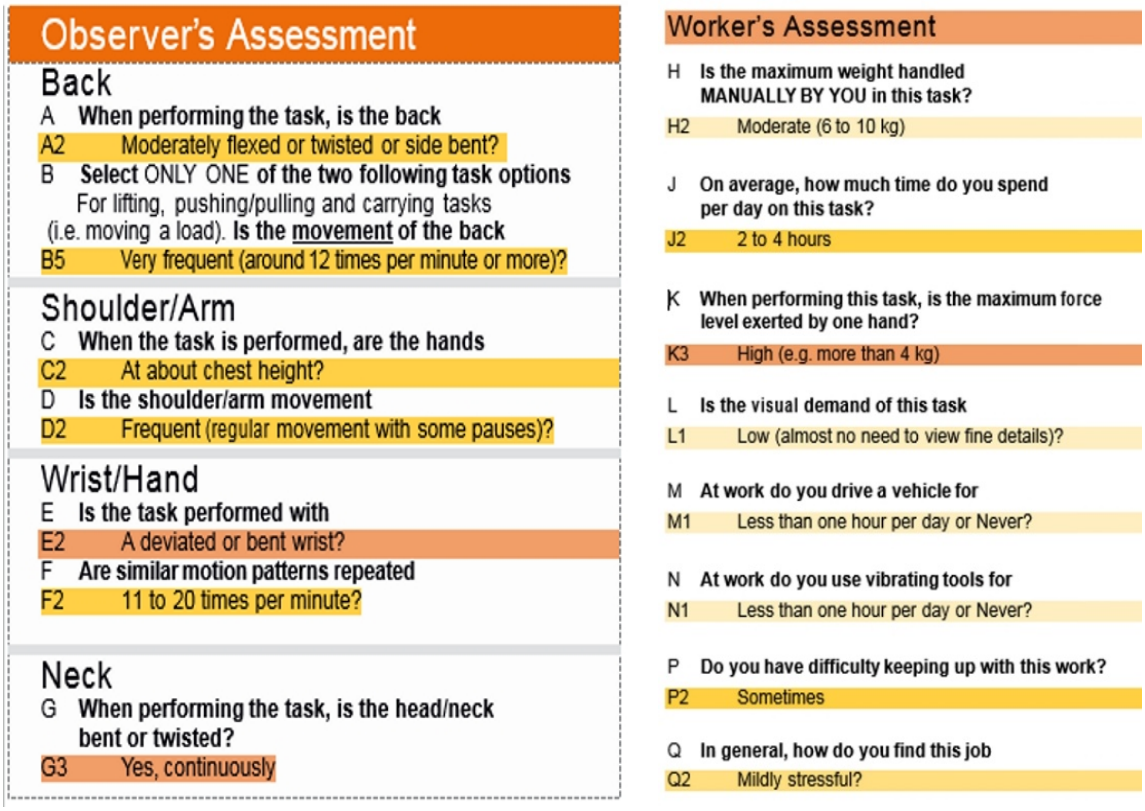

(a) (b)

FIG. 4. (a) Observer's assessment, (b) Worker's assessment

The evaluation form shown in Figure 4 shows values for different parts of the body, which, if correlated, can provide a clearer picture of the effort that the worker's body puts into carrying out this activity.

For example, for the back, although we are in situation A2, in conjunction with B5, which means that the movement of the back in these positions is very frequent, it is understood that the worker's back is overloaded when performing this activity.

A similar situation characterizes the wrist/hand, because in most cases where parts are handled, the wrists are flexed close to the natural limit, thus causing great tension in the muscles, tendons, ligaments. At the same time, the neck is almost permanently turned and tilted, especially when placing the pieces in the trolley, and at the base of the trolley, because it has to bend even further, while looking for the right place to place the piece. These related aspects justify the workers' response that sometimes they can't keep up with the pace at work and that the respective activity creates quite a lot of physical and mental stress for them.

Fig. 5 shows the evaluation by means of the RULA method of the same working position.

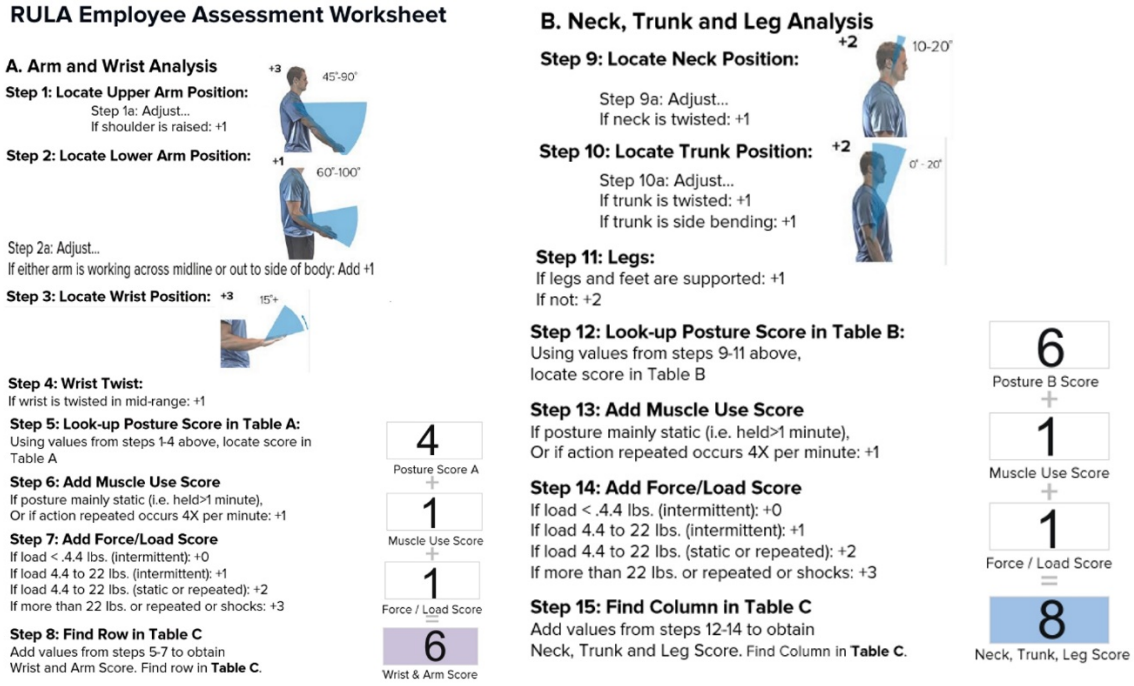

FIG. 5. RULA assessment worksheet

Figure 5 shows the results obtained by applying the RULA method for the same activity. Of course, the scores and the approach are specific to the RULA method and differ slightly from the QEC method scores, but, in principle, the results should lead to similar conclusions. From the calculation of scores while applying the RULA method, quite a few similarities can be observed in relation to the results obtained by the QEC method, as shown below.

4. RESULTS

As part of the risk assessment, a number of 14 workers were analyzed for this activity. Table 2 shows the important characteristics of these workers, compared to the requests they are exposed to, when they perform this activity.

Table 3. The characteristics of the evaluated workers

No	Man/ Woman (M / W)	Height (cm)	Age (years)	Experience in this activity (months)	The physical condition of the worker (Athletic, Good, Weak)
1	M	172	28	22	A
2	M	170	31	14	G
3	M	168	28	28	G
4	M	181	42	32	G
5	W	157	38	14	G
6	W	163	27	14	G
7	M	172	25	22	A
8	W	166	27	22	W
9	M	181	30	26	A
10	M	175	44	28	W
11	W	162	30	20	G
12	M	168	49	32	G
13	M	178	32	18	W
14	M	174	29	26	G

The physical condition of the worker during an activity, especially if the respective activity involves physical effort (e.g. manipulation of masses), or postural effort (e.g. standing, bent trunk), or combined efforts, is an important factor in ergonomics, because the same effort under the same conditions is perceived and felt very differently by the worker if they have a good physical condition or not (if the worker is tall or short, if they have more or less physical strength, etc.), or if they possess more or less developed skills to face this effort. For these reasons, the physical condition of the workers was recorded.

Using the calculation tables specific to the RULA method, the resulting final score is 7, which according to Table 4, represents the maximum score.

Table 4. Scoring: final score from Table C

Scoring	Actions
1 - 2	acceptable posture
3 - 4	further investigation, change may be needed
5 - 6	further investigation, change soon
7	investigate and implement change

In order to be able to compare the results of the two methods QEC and RULA, a correspondence table (Table 5) of the results of the two methods is needed.

Table 5. Correspondence matrix

Risk level	QEC-Exposure Score (E)	RULA
1	≤ 40%	1 - 2
2	41 – 50%	3 - 4
3	51 – 70%	5 - 6
4	> 70%	7

By replacing in equation (1) the data obtained by means of the QEC questionnaire and from the tables containing the exposure scores, presented in equation (2), a final score of 122 results, which means an exposure of 69.32%, which is very close to the level of maximum risk.

$$E(\%) = \frac{X}{X_{max}} x100\% = \frac{122}{176} x100\% = 69{,}32\% \quad (2)$$

Analyzing the results obtained by the two methods QEC and RULA and taking into account the table of correspondence (Table 5), it is found that the results obtained by using the two methods are broadly similar, but still differ to a certain extent.

5. DISCUSSION

As shown, although they are easy to use and lead to quite accurate results, the QEC and RULA methodologies can sometimes lead to different results or conclusions, because they do not take into account a number of factors or ergonomic working conditions that can affect, in many situations, the state of health of the workers.

Although the methods used in the evaluation of ergonomic risks for conveyor belt activity, QEC and RULA, lead to close diagnoses, and in the particular case analyzed, to a high level of risk, and it is considered that these methods are fast and offer a degree of precision of acceptable diagnosis, however, due to the fact that these methods (as well as others) for evaluating ergonomic risks do not take into account the physical condition of the worker (except to a small extent and indirectly), they can even give an erroneous diagnosis of the situation evaluated from ergonomic point of view. In the cases evaluated in this study, these aspects were taken into account, so that, based on the resulting diagnosis, appropriate remedial measures can be proposed, to avoid affecting the health and safety of the workers.

In order to compensate to some extent for the said limitations of the assessment methods, the experience of risk assessors in the ergonomic analysis of the entire work situation is particularly necessary.

CONCLUSIONS

The position of the worker's body influences their efficiency in the conveyor belt activity, and this also emerges from the evaluation results, which show that the operator's risk level score at the workplace is 3 (QEC) and 4 (RULA), but these values are very close. Based on the results obtained from the QEC&RULA analysis, it can be observed that the Exposure Level perceived by the worker is quite high, so that the worker's posture requires immediate improvement. A good posture of the worker definitely leads to an increased work productivity. Comparisons between methods showed a positive association between QEC and RULA, so we recommend using these two methods simultaneously to assess the posture of workers in similar tasks.

In conclusion, this study showed that workers who move parts from the conveyor belt to the trolley and vice versa are at risk of WMSD and improving risk control may involve the implementation of appropriate ergonomic training and education programs for workers. Also, the results of the present study indicate the need to implement preventive programs in the industrial environment to control those risks that lead to more severe musculoskeletal disorders in workers.

In order to investigate in more detail some causes of musculoskeletal disorders in workers, additional investigations are needed, depending on the type of conveyor belt, its height and the height of trolleys, as well as the position of the worker in relation to the conveyor belt and the trolley.

In this sense, our current and future research aims to improve these methods by adding certain elements that in practice have a substantial impact on ergonomics and on the health of the workers. For example, in addition to the height of the work plane compared to the height of the worker, most of the time, in reality, the physical condition of the worker when performing the respective activity or the conditions of the work environment, such as the ambient temperature in which the activity is carried out, also matter, because a low temperature can obviously have a greater impact on the worker's health, especially if the body is not previously prepared to exert effort in these conditions.

REFERENCES

[1] R. Brown, G. Li and P. T. McCape, *Contemporary Ergonomics*, Taylor & Francis, London 2003;
[2] G. David, V. Woods, G. Li and P. Buckle, The development of the Quick Exposure Check (QEC) for assessing exposure to risk factors for work-related musculoskeletal disorders, *Applied Ergonomics*, vol. 39, no. 1, pp. 57-69, 2008;
[3] S. Oliv, E. Gustafsson, A. N. Baloch, M. Hagberg and H. Sandén, The Quick Exposure Check (QEC) - Inter-rater reliability in total score and individual items, *Applied Ergonomics*, vol. 76, pp. 32-37, 2019.
[4] A. S. K. Cheng and P. C. W. So, Development of the Chinese version of the Quick Exposure Check (CQEC), *Work*, vol. 48, no. 4, pp.503-510, 2014;
[5] P. Ericsson, M. Björklund and J. Wahlström, Exposure assessment in different occupational groups at a hospital using Quick Exposure Check (QEC) – A pilot study, *Work*, vol. 41, pp. 5718-5720, 2012;
[6] L. McAtamney and E. N. Corlett, RULA: a survey method for the investigation of work-related upper limb disorders, *Applied Ergonomics*, vol. 24, no. 2, pp. 91-99, 1993;
[7] J. Singh, H. Lal and G. Kocher, Musculoskeletal Disorder Risk Assessment in small scale forging Industry by using RULA Method, *International Journal of Engineering and Advanced Technology (IJEAT)*, vol.1, no. 5, pp. 513-517, 2012;
[8] M. J. Sanders, *Ergonomics and the Management of Musculoskeletal Disorders*, 2nd Edition, Butterworth-Heinemann Books-Elsevier, Oxford, 2003;
[9] N. Jaffar, A. H. Abdul-Tharim, I. F. Mohd-Kamar and N. S. Lop, A Literature Review of Ergonomics Risk Factors in Construction Industry, *Procedia Engineering*, vol. 20, pp. 89-97, 2011;
[10] J.R. Ayu Bidiawati and E. Suryani, Improving the Work Position of Worker's Based on Quick Exposure Check Method to Reduce the Risk of Work Related Musculoskeletal Disorders, *Procedia Manufacturing*, vol. 4, pp. 496-503, 2015;
[11] H. Y. Kohammadi, Y. Sohrabi, M. Poursadeghiyan, R. Rostami, A. Rahmani Tabar, D. Abdollahzadeh and F. Rahmani Tabar, Comparing the Posture Assessments Based on RULA and QEC Methods in a Carpentry Workshop, *Research Journal of Medical Sciences*, vol. 10, no. 3, pp 80-83, 2016;
[12] D. Kee, Systematic Comparison of OWAS, RULA, and REBA Based on a Literature Review, *International Journal of Environmental Research and Public Health*, vol. 19, no. 1, pp. 595, 2022.

STUDY ON THE INFLUENCE OF TREATMENT PARAMETERS ON THE HARDNESS OF 6XXX SERIES ALUMINIUM ALLOYS

Maria STOICANESCU
"Transilvania" University of Brasov, Romania (stoican.m@unitbv.ro)
ORCID: 0000-0003-3138-1830

DOI: 10.19062/1842-9238.2023.21.1.7

Abstract: *The appropriate application of heat treatments results in structural changes in alloys, and such changes enable the improvement of strength, hardness, ductility and other mechanical characteristics. This paper is mainly aimed at studying and analysing the influence of the quenching temperature and of the ageing holding time on the hardness of 6xxx series aluminium alloys. The thermal processes and parameters involved in the heat treatment of this alloy are studied, such as quenching and ageing, and the manner in which these treatments influence the properties of the resulting materials will be investigated.*

Keywords: *6xxx series Al alloys; heat treatment; microstructure*

1. INTRODUCTION

Aluminium alloys are becoming a more prominent area of research and development in modern industry [1]. Due to their outstanding properties, such as corrosion resistance, ease of processing and low density, aluminium alloys are used in a wide range of industrial applications [2,3]. From the aeronautical and automotive industries to construction and packaging, aluminium alloys offer innovative and economical technical solutions. 6xxx series aluminium alloys are known for their excellent mechanical strength and corrosion resistance properties [4,5,6]. The heat treatment of these alloys is essential for obtaining the desired properties and for optimizing their performance.

2. EXPERIMENTAL RESEARCH

The material used in the experimental tests was 6082 series aluminium alloy.
The chemical composition for the material used is presented in table 1:

Table 1. Chemical composition

Si	Fe	Cu	Mn	Mg	Cr	Zn	Ni	Ti	Al
1,09	0,35	0,08	0,67	0,98	0,14	0,07	0,01	0,03	balance

The alloy en aw-6082 is a high strength alloy for highly loaded structural applications. Due to the fine grained structure this alloy exhibits a good resistance to dynamic loading conditions. En aw-6082 is certified for use in marine applications.

6082 series aluminium alloy samples were used for the study, and they were divided into 3 working variants - quenching temperatures and different ageing holding times.

Variant 1

For the first variant, the samples were heated to 530 °C, held for 30 minutes and cooled in water.

After quenching, the samples were aged at 177°C for different holding times, i.e. 30 minutes and 1 hour.

1. Sample 1 was aged at 177 °C, held at this temperature for 30 minutes and cooled in air.

2. Sample 2 was aged at 177 °C, held at this temperature for 1 hour and cooled in air.

Variant 2

For the second variant, the samples were heated for quenching to 540 °C and held at this temperature for 30 minutes, cooled in water, and artificially aged at 177°C for different holding times.

3. Sample 3 - aged at 177 °C, held for 30 minutes and cooled in air.

4. Sample 4 - aged at 177 °C, held for one hour and cooled in air.

For the third variant, the samples were heated for quenching to 550 °C and held at this temperature for 30 minutes, cooled in water, and artificially aged at 177°C for different holding times.

5. Sample 5 - aged at 177 °C, held for 30 minutes and cooled in air.

6. Sample 6 - aged at 177 °C, held for 1 hour and cooled in air.

After applying the treatment presented above, the hardness of each sample was measured and they were embedded in resin for microscopic analysis.

Table 2 shows the hardness values obtained.

Table 2 Treatment conditions and hardness values obtained

Sample	Heat treatment			Brinell Hardness	
	Quenching temperature [°C]	Ageing temperature [°C]	Holding time [h]	Footprint diameter	Hardness [HB]
1	530	177	0.5	1.10	62.4
2			1	1.08	64.9
3	540	177	0.5	0.97	81.3
4			1	0.93	112
5	550	177	0.5	1.03	71.7
6			1	0.98	79.5

An increase in hardness was obtained for the treatment carried out at a temperature of 540°C/30 min/water followed by ageing at 177°C, for both holding times, i.e. 30 minutes and 1 hour, cooled in air.

Table 1 shows the variation in hardness for the applied heat treatment variants. The hardness value recorded for Sample 4 is higher in relation to the rest of the parts.

Following the heat treatment, all samples were ground, polished and etched, after which they were studied under a microscope.

Figure 1 shows the metallographic structure after annealing (initial state), and a uniform distribution of the components as well as a high porosity can be observed. No inclusions were identified in the analysed samples.

FIG. 1 Metallographic structure after annealing (in the initial state). HF etching. 100X magnification

Figure 2 shows the metallographic structure obtained by quenching from 540 °C, holding for 30 minutes and cooling in water.

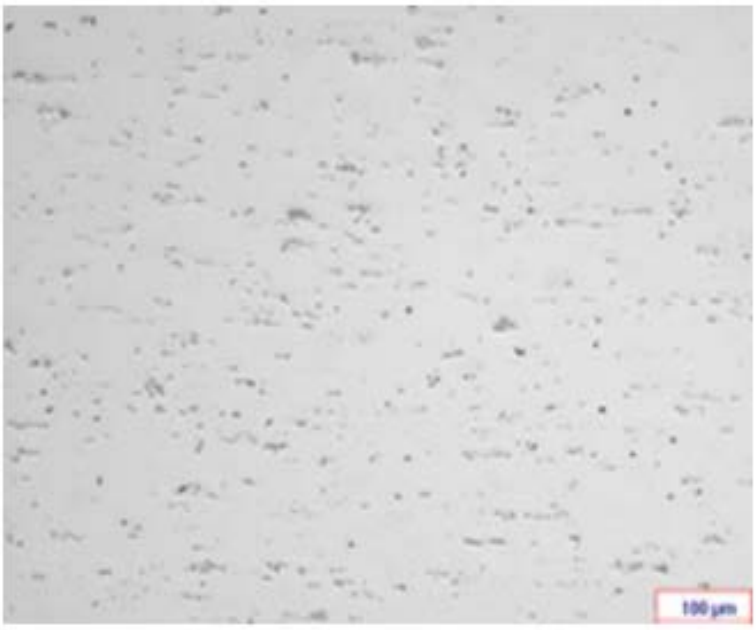

FIG. 2 Metallographic structure after quenching from 540 °C, holding for 30 minutes, cooling in water. HF etching. 100X magnification

Figure 3 shows the metallographic structure obtained by quenching from 550 °C, holding for 30 minutes and cooling in water.

FIG. 3 Metallographic structure after quenching from 550 °C, holding for 30 minutes and cooling in water. HF etching. 100X magnification

The figures above show the gas pores and the basic metallic mass.

Figures 4 and 5 show the metallographic structures after the quenching and ageing heat treatment offering the best hardness values.

FIG. 4 Metallographic structure after quenching at 540 °C, 30 minutes/water and ageing at 177 °C for 30 minutes HF etching. 100X magnification

FIG. 5 The metallographic structure after quenching at 540 °C, 1 h/water and ageing at 177 °C for one hour. HF etching. 100X magnification.

Fine dispersed precipitates of Mg2Si can be observed in the analysed structures.

CONCLUSIONS

The 530 °C heating temperature for quenching shows that it was not high enough and no ageing hardening occurred.

The samples treated according to the structures in Figures 4 and 5 show a substantial increase in hardness.

The heat treatments the structures of which are shown in figures 4 and 5 feature the highest hardness values from the range of analysed heat treatments.

The 550 °C temperature selected for quenching is reasonable considering the hardness results obtained after ageing.

In all cases, the increase of the holding time to one hour led to higher hardness values regardless of the heating temperature for quenching.

The hardening phase of these alloys is the -Mg2Si phase, which precipitates during cooling.

Very fine Mg2Si dispersed precipitates can be observed in the structures obtained.

No inclusions were identified in the analysed samples.

REFERENCES

[1] W. S. Miller, L.Zhuang, J. Bottema, A. J. Wittebrood, P. De Smet, A. Haszler, A. Vieregge, *Recent development in aluminium alloys for the automotive industry*. Materials Science and Engineering: A, 280(1), 37–49, 2000, https://doi.org/10.1016/S0921-5093(99)00653-X ;

[2] Jaradeh, Majed. *The Effect of Processing Parameters and Alloy Composition on the Microstructure Formation and Quality of DC Cast Aluminium Alloys*. Doctoral thesis, KTH, Materialvetenskap, 2006, http://urn.kb.se/resolve?urn=urn:nbn:se:kth:diva-4205;

[3] G. Al-Marahleh, *Effect of heat treatment on the distribution and volume fraction of Mg2Si in structural aluminum alloy 6063*. Met Sci Heat Treat 48, 205–209, 2006. https://doi.org/10.1007/s11041-006-0071-5;

[4] P. Priya, *Microstructural evolution during the homogenization heat treatment of 6XXX and 7XXX aluminum alloys*. PhD Thesis. Purdue University, 2016, https://docs.lib.purdue.edu/cgi/viewcontent.cgi?article=2203&context=open_access_dissertations ;

[5] H.Danesh Manesh, A. Karimi Taheri *The effect of annealing treatment on mechanical properties of aluminum clad steel sheet*. Materials & Design, ISSN 0261-3069, Volume 24, Issue 8, Pages 617-622, 2003, https://doi.org/10.1016/S0261-3069(03)00135-3;

[6] Niels C. W Kuijpers, F. Vermolen, C. Vuik, S. Zwaag, *A model of the β-AlFeSi to α-Al(FeMn)Si transformation in Al-Mg-Si alloys*. MATERIALS TRANSACTIONS. 44, Pp.1448-1456, 2003, https://doi.org/10.2320/matertrans.44.1448.

SPACE DOMAIN AWARENESS AND CRITICAL SPACE INFRASTRUCTURES: IMPLICATIONS FOR AIRSPACE GEOPOLITICS

Ulpia-Elena BOTEZATU
Romanian Space Agency, Bucharest, Romania (ulpia.botezatu@rosa.ro)
National Institute for Research & Development in Informatics - ICI Bucharest, Romania
ORCID: 0000-0002-9879-0500

DOI: 10.19062/1842-9238.2023.21.1.8

Abstract: *This interdisciplinary scientific article explores the dynamic intersection of Space Domain Awareness (SDA) and Critical Spatial Infrastructures (CSI), as well as their far-reaching implications for airspace geopolitics. With the increasing reliance on space assets and the growing interest in space exploration, ensuring a comprehensive understanding of the space domain becomes crucial for safeguarding critical spatial infrastructures and maintaining regional geopolitical stability. This article delves into the challenges and opportunities arising from the interplay between SDA and CSI, shedding light on the complex relationships that shape airspace security and geopolitics.*

Keywords: *Space Domain Awareness, Critical Space Infrastructures, Airspace Geopolitics, Space Assets, Surveillance and Tracking, Space Situational Awareness, Geopolitical Stability, Space Security*

1. INTRODUCTION

The utilization of space for civilian, commercial, and military purposes has experienced a spectacular rise, revolutionizing the way we interact with the world and driving significant advancements in technology and science. This exponential growth has brought about an ever-increasing dependence on space assets, making them indispensable to modern society. Those Space Infrastructures (SI) that are *critical* integrators for other strategic domains include a wide array of space-based assets and ground-based facilities, and have become the backbone of numerous essential services that impact virtually every aspect of human life [1].

Space assets play a pivotal role in providing vital services such as global communication, precise navigation systems, real-time weather monitoring, and reconnaissance for national security and defense. From satellite-based communication networks facilitating instant global connectivity to Global Positioning System (GPS) satellites enabling accurate location-based services, the seamless functioning of these critical spatial infrastructures is vital for supporting economic activities, ensuring public safety, and enhancing military capabilities [1, 2, 3, 4].

However, the rapid growth of space activities has led to an increasingly congested and contested space domain [5]. The proliferation of satellites and other space debris has significantly heightened the risk of collisions, posing a serious threat to existing space assets [6]. Additionally, advancements in technology have given rise to new challenges, including potential cyber-attacks and electromagnetic interference that could disrupt the normal functioning of critical spatial infrastructures [7].

The vulnerability of these assets to both natural hazards, such as solar storms and cosmic radiation, and human-made hazards, such as intentional satellite disruptions or space-based aggression, demands urgent attention.

To safeguard the integrity and functionality of these crucial infrastructures, effective Space Domain Awareness (SDA) has become an imperative. Space Domain Awareness involves the continuous monitoring, tracking, and understanding of objects and activities in space [8, 9]. By maintaining situational awareness of the space domain, space agencies and governments can identify potential threats, anticipate collisions, and respond promptly to any anomalies or suspicious activities. Timely detection and response are essential to mitigating risks and ensuring the safety and security of critical spatial infrastructures.

Therefore, the focus on Space Domain Awareness, particularly when considered in a broader correlation with Critical Spatial Infrastructures, has grown significantly. An integrated approach that combines technological advancements, international cooperation, and policy frameworks is essential to addressing the multifaceted challenges posed by the growing space activities. By fostering collaboration among spacefaring nations and organizations, we can collectively enhance Space Domain Awareness and promote responsible space practices to mitigate potential conflicts and safeguard critical spatial infrastructures for the benefit of all humanity. This article aims to explore the complex relationships between Space Domain Awareness and Space Critical Infrastructures, shedding light on their implications for airspace geopolitics and the broader global landscape.

2. UNDERSTANDING SPACE DOMAIN AWARENESS (SDA)

This section provides an in-depth analysis of Space Domain Awareness (SDA), a critical component in comprehending the dynamic and complex environment of the space domain. SDA involves a comprehensive set of technologies, methodologies, and data sources utilized to monitor, track, and analyze objects and activities within space. By continually observing and evaluating objects such as satellites, spacecraft, debris, and potential threats, SDA plays a pivotal role in enhancing the safety and security of space critical infrastructures and other space assets [8, 9].

A key aspect emphasized in this section is the paramount importance of space situational awareness in space (SSA) operations. SDA enables stakeholders to maintain real-time awareness of the space environment, including the precise location, trajectory, and characteristics of space objects. This heightened awareness is indispensable for space agencies, governments, and private entities to make informed decisions regarding satellite launches, orbital maneuvers, and mission planning, thus minimizing the risk of collisions and optimizing space asset utilization.

Surveillance and Space Situational Awareness (SSA) activities and network of organizations are pivotal players in bolstering the effectiveness of SDA. These organizations continuously collect data from a variety of sources, such as ground-based radars, space-based sensors, and satellite tracking networks. They consolidate this information to create accurate and up-to-date catalogs of space objects, identifying potential conjunctions and collision risks, and providing essential early warnings for potential space debris-related hazards.

Romania has played a pivotal role in the EU Space Surveillance and Tracking (SST) Partnership [10], demonstrating a proactive commitment to enhancing space situational awareness and bolstering the region's capabilities in space domain monitoring.

As a member of the European Union and a participant in space-related activities, Romania has actively engaged in collaborative efforts to advance the SST initiative. Through participation in joint projects, data-sharing agreements, and technological advancements, Romania has contributed valuable insights and resources to support the EU's objective of fostering a safer and more secure space environment. By leveraging its expertise in aerospace research and technology, Romania continues to make significant strides in the field of Space Domain Awareness, making essential contributions to the EU's collective efforts to track and monitor space objects, prevent collisions, and address potential threats to critical space infrastructure. As the SST Partnership evolves, Romania's active involvement reaffirms its commitment to international cooperation and proactive space governance, further cementing its position as a key player in European space endeavors.

The exponential growth of space debris presents one of the most pressing challenges for SDA [11]. Discarded rocket stages, defunct satellites, and other fragments pose significant risks to operational spacecraft and critical spatial infrastructures. This section delves into the complexities of tracking and monitoring space debris, including the assessment of potential conjunctions between objects. Advanced algorithms and computational models are crucial for predicting and mitigating potential collisions, as well as for devising optimal collision avoidance strategies to safeguard valuable space assets.

In light of these challenges, the need for effective SDA frameworks becomes evident. Collaborative efforts between governments, international space agencies, and private industry are vital for sharing data and expertise, thus fostering a robust SDA ecosystem . Additionally, investments in research and development are essential to enhance the accuracy and scope of SDA capabilities, promoting the sustainability of space activities and reinforcing the protection of critical spatial infrastructures.

Overall, this section underscores the vital role of SDA in shaping the future of space exploration and utilization. The integration of advanced technologies, methodologies, and surveillance systems within the realm of SDA enhances our ability to navigate the increasingly congested and contested space domain. By effectively managing space debris, mitigating collision risks, and promoting collaborative frameworks, SDA paves the way for the secure and prosperous growth of critical spatial infrastructures and the broader space industry.

3. CRITICAL SPACE INFRASTRUCTURES AND AIRSPACE GEOPOLITICS

This section delves into the profound significance of critical spatial infrastructures (CSI), which comprise a diverse array of space-based assets and ground-based facilities. CSI play a pivotal role in modern societies, enabling crucial functions such as global communication, precise navigation, climate monitoring, earth observation, and national security operations. As an indispensable backbone of various economic sectors, disruptions to these infrastructures can have far-reaching consequences that extend beyond individual nations and can impact the global community.

The analysis begins by examining the economic ramifications of potential disruptions to CSI. Given the immense reliance on satellite-based communication and navigation systems in the global economy, any interruptions in these services could lead to severe financial losses and hamper international trade. Disruptions in earth observation and climate monitoring capabilities could also adversely affect agriculture, disaster management, and environmental protection efforts, with dire consequences for both developed and developing nations.

Moreover, disruptions to critical spatial infrastructures can have significant societal impacts. Emergency response systems that depend on satellite-based communication might suffer delays or incapacitation during crises, potentially leading to increased casualties and damage. Additionally, disruptions in satellite-based internet services could adversely affect education, healthcare, and disaster relief in remote and underserved regions.

From a military perspective, the vulnerability of CSI raises concerns regarding national security. Space-based assets play a critical role in military operations, including reconnaissance, communication, surveillance, and missile warning systems. Any hostile actions against these assets could severely undermine a nation's defense capabilities, leading to potential regional destabilization or escalation of conflicts.

The geopolitical implications of airspace control and surveillance further underscore the significance of critical spatial infrastructures. Nations strategically leverage their spatial assets to gain advantages over rivals, asserting dominance in specific regions and projecting power globally. The ability to monitor adversaries' activities through space-based surveillance provides valuable intelligence, shaping military and diplomatic decisions. As a result, airspace geopolitics emerge as a complex interplay of national interests, alliances, and potential flashpoints, influencing the dynamics of international relations.

Given the increasing militarization and commercialization of space, it becomes imperative for nations to safeguard their critical spatial infrastructures and maintain their access to space for peaceful purposes. International cooperation and adherence to space law play crucial roles in managing airspace geopolitics, preventing conflict escalation, and fostering space sustainability. Consequently, understanding the intricate interdependencies between critical spatial infrastructures, airspace geopolitics, and international relations is vital for navigating the challenges and opportunities presented by the space domain in the 21st century.

4. THE CONFLUENCE OF SDA AND CSI: SECURING AIRSPACE GEOPOLITICS

The third section delves into the dynamic interplay between Space Domain Awareness (SDA) and Critical Spatial Infrastructures (CSI) and their combined role in maintaining regional airspace geopolitics. By understanding and harnessing the synergies between these domains, nations can bolster their capacity to safeguard essential assets in space and on the ground.

Enhanced space domain awareness plays a pivotal role in strengthening the protection of critical spatial infrastructures against an array of emerging threats. Space-based aggression is an escalating concern, as nations seek to gain a competitive edge by targeting adversaries' satellites or deploying anti-satellite capabilities. An in-depth understanding of the space domain's dynamics and constant surveillance can enable timely response and deterrence measures, reducing the vulnerability of critical space assets to potential acts of aggression.

Additionally, the increasing dependence on interconnected networks and information technologies exposes critical spatial infrastructures to cyber-attacks. Hostile actors might attempt to disrupt satellite communications, compromise ground-based systems, or manipulate data to cause widespread chaos and disruptions. Combining space domain awareness with robust cybersecurity measures can build resilience and mitigate the impact of cyber threats, ensuring the continuity of critical services and preserving regional stability.

Moreover, the section addresses the significance of mitigating electromagnetic interference (EMI) within the space domain. The proliferation of space assets and the rise of mega-constellations introduce challenges related to radio frequency interference. Ensuring uninterrupted access to radio frequency spectrum is crucial for the optimal functioning of critical spatial infrastructures and avoiding clashes between satellite systems. A comprehensive space domain awareness approach helps identify and address EMI sources, enabling effective spectrum management and reducing potential conflicts between space operators.

Furthermore, the confluence of SDA and CSI necessitates international collaboration and information sharing among nations to foster collective security in the space domain. As space becomes more congested and contested, the need for cooperation and transparency becomes increasingly apparent. Sharing tracking data, conjunction assessments, and other relevant space-related information can facilitate improved situational awareness, reducing the risks of accidental collisions or misunderstandings between space actors [12].

Promoting responsible space behavior and adherence to international norms and agreements is also a critical aspect of securing airspace geopolitics. Encouraging all spacefaring nations to abide by guidelines such as the United Nations Space Debris Mitigation Guidelines or the Code of Conduct for Outer Space Activities can promote responsible and sustainable space practices, minimizing the generation of space debris and the potential for space-related conflicts.

In conclusion, the confluence of Space Domain Awareness and Critical Spatial Infrastructures offers significant opportunities for enhancing airspace geopolitics and space security. By leveraging advanced technologies and fostering international cooperation, nations can effectively protect their critical space assets from emerging threats, bolster regional stability, and ensure the sustainable use of space resources for the benefit of humanity. A proactive and collaborative approach will be pivotal in navigating the challenges of an increasingly complex and interconnected space domain.

CONCLUSIONS

In the face of ever-increasing space activities and the growing importance of space assets in diverse sectors, the interplay between Space Domain Awareness (SDA) and Critical Spatial Infrastructures (CSI) emerges as a complex and multifaceted domain that significantly impacts airspace geopolitics. As nations endeavor to bolster their space capabilities and protect their strategic interests, it becomes imperative to grasp the intricate dynamics at the intersection of SDA and CSI. This understanding is vital for fostering regional stability and ensuring the sustainable utilization of space resources.

With the escalating utilization of space for communication, navigation, remote sensing, and national security, the protection of critical spatial infrastructures becomes a top priority for governments and organizations alike. These infrastructures comprise an amalgamation of space-based assets, ground stations, data centers, and associated networks, all playing pivotal roles in facilitating modern life. Yet, they face a range of potential risks, including collisions with space debris, cyber-attacks, intentional interferences, and natural space phenomena. Effective Space Domain Awareness plays a critical role in mitigating these risks by providing real-time data on the location and behavior of space objects, facilitating early warning systems, and guiding collision avoidance measures.

The link between SDA and CSI further extends to airspace geopolitics, where nations assert control over their territories and airspace to safeguard their interests. Geopolitical rivalries in the space domain can manifest in disputes over orbital slots, spectrum allocation, and the positioning of critical spatial infrastructure facilities. Heightened international competition in space exploration and exploitation underscores the significance of airspace control and surveillance, with strategic advantages at stake for nations possessing advanced SDA capabilities.

To navigate the intricate challenges and seize the opportunities arising from the interdisciplinarity of SDA and CSI, international cooperation stands as a paramount principle. Collaborative efforts among nations can facilitate the sharing of space situational awareness data, intelligence, and best practices, promoting collective security and reducing the risk of misunderstandings or conflicts in the space domain. Establishing clear policy frameworks, agreements, and norms of behavior for space activities can bolster predictability and promote responsible behavior, fostering an environment conducive to peace and cooperation.

Furthermore, technological advancements play a crucial role in enhancing SDA capabilities and bolstering the resilience of critical spatial infrastructures. Research and development efforts should focus on innovative sensing technologies, artificial intelligence, and data analytics to improve space object tracking and situational awareness accuracy. Emphasizing the standardization and compatibility of space-based systems can promote interoperability and data exchange among different nations and organizations, thereby fostering a safer and more secure space environment.

Ultimately, the successful convergence of SDA and CSI can contribute to ensuring regional stability, averting potential airspace conflicts, and fostering the sustainable and peaceful utilization of space resources for future generations. By recognizing the interdependence of these fields and prioritizing international collaboration, policy coherence, and technological innovation, the global community can navigate the evolving landscape of airspace geopolitics while safeguarding critical spatial infrastructures in an increasingly interconnected and space-dependent world.

REFERENCES

[1] U.E. Botezatu, Piso, M. I. (2020), *Vital Outer Space Infrastructures: Romania's Pursuits and Achievements*, in Unal Tatar, Adrian V. Gheorghe, Omer F. Keskin, Jean Muylaert, *Space Infrastructures: From Risk to Resilience Governance*, ISBN 978-1-64368-072-9 (print) | 978-1-64368-073-6 (online), pp. 329 – 336, DOI 10.3233/NICSP200033;

[2] M. I. Piso, (2020), *Space Systems as Critical Infrastructure*, International Academy of Astronautics.

[3] O. Bucovetchi, U.E. Botezatu, R. Stanciu , (2020) *Security of Space and Critical Infrastructures*, Proceedings of the 36th IBIMA Conference: 4-5 November 2020, Granada, Spain;

[4] A. Georgescu, U.E. Botezatu, A.-D. Popa, Ș. Popa, Ș.-C. Arseni, (2016) *Critical infrastructure dependency on space systems*, "Mircea cel Batran" Naval Academy Press, Constanta, Romania, "Mircea cel Batran" Naval Academy Scientific Bulletin, Volume XIX – 2016 – Issue 1;

[5] *** *EU Space Strategy for Security and Defence: for a stronger and more resilient European Union*, available online at: https://defence-industry-space.ec.europa.eu/eu-space-policy/eu-space-strategy-security-and-defence_en, last accessed August 1, 2023;

[6] R. Buchs, (2021). *Collision risk from space debris: Current status, challenges and response strategies*. Lausanne: EPFL International Risk Governance Center. DOI: 10.5075/epfl-irgc-285976;

[7] U.E. Botezatu, Attempted Cyber Security of Systems and Operations in Outer Space: an Overview of Space-based Vulnerabilities, *Romanian Cyber Security Journal*, ISSN 2668-6430, vol. 5(1), pp. 67-76, 2023. DOI:10.54851/v5i1y202306;

[8] D. L. Oltrogge, S. Alfano, C. Law, A. Cacioni and T. S. Kelso, A comprehensive assessment of collision likelihood in Geosynchronous Earth Orbit, *Acta Astronautica*, vol. 147, pp. 316–345, 2018. doi:10.1016/j.actaastro.2018.03.017;

[9] B. Weeden & V. Samson, (Eds.). (2020), *Global Space Governance: An International Study*. Springer International Publishing;
[10] European Union. (2021) Space Surveillance and Tracking (SST) [online] https://www.eusst.eu/ ;
[11] 28 July 2022, Defense Invation Unit, Commercial Space Industry Providing Tools To Advance and Augment Space Domain Awareness Visualization and Analytics [online] https://www.diu.mil/latest/commercial-space-industry-providing-tools-to-advance-and-augment-space;
[12] 14 April 2022, SpaceNews, Space domain awareness: A secret weapon against shadowy threats in orbit, [online] https://spacenews.com/space-domain-awareness-a-secret-weapon-against-shadowy-threats-in-orbit/.